Imaging with Coherent X-rays

Review: Optical Coherence

Temporal Coherence

Ability of a light beam to form fringes with a delayed version of itself

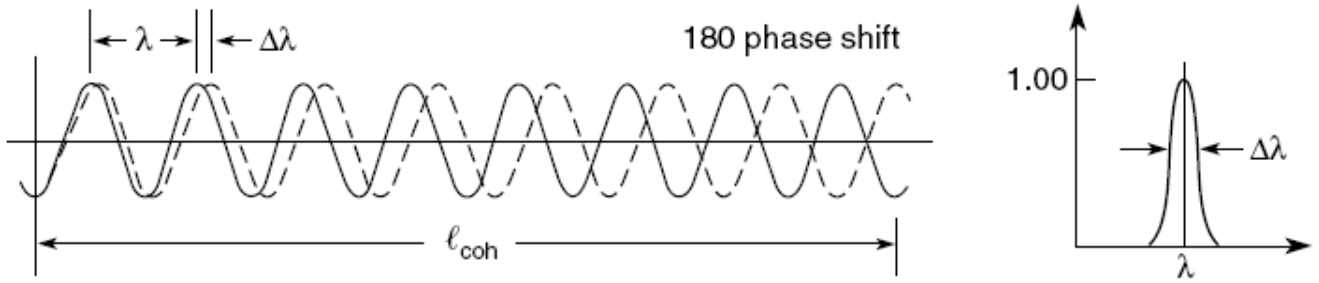

Spatial Coherence

Ability of spatially separated points in a wavefront to form fringes.

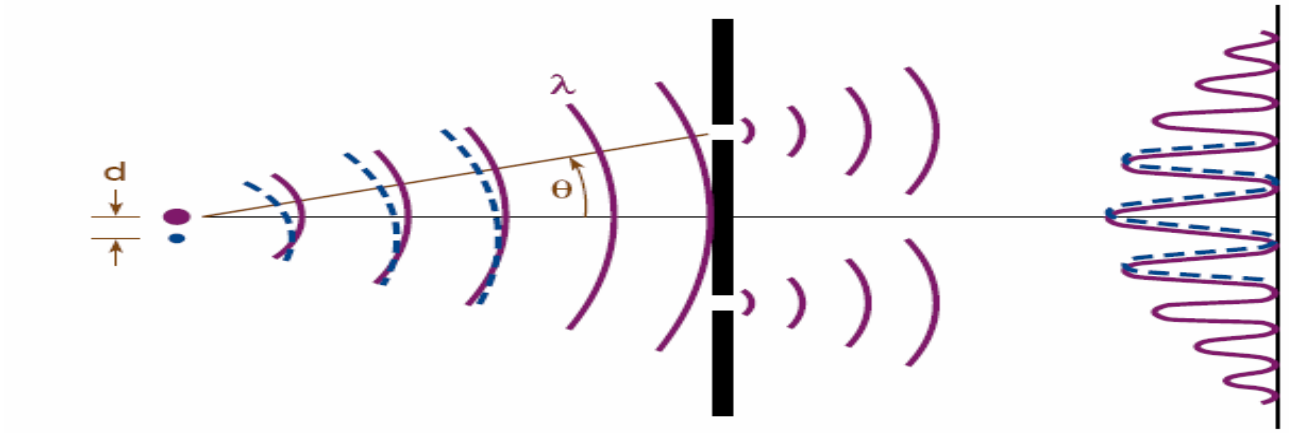

Temporal Coherence

Temporal Coherence

Ability of a light beam to form fringes with a delayed version of itself.

Example

We have an undulator with N = 55 periods, and we tune it to 2.4 nm.

$$\lambda_0 = 2.4nm$$

Recall that spectral bandwidth is proportional to the number of periods in the undulator N:

$$\frac{\Delta\lambda}{\lambda_0} = \frac{1}{N} = \frac{1}{55}$$

Electric field of a quasimonochromatic x-ray pulse with finite bandwidth

What does the electric field look like from a single electron radiator?
Assume it is a perfect point source.

Frequency Domain

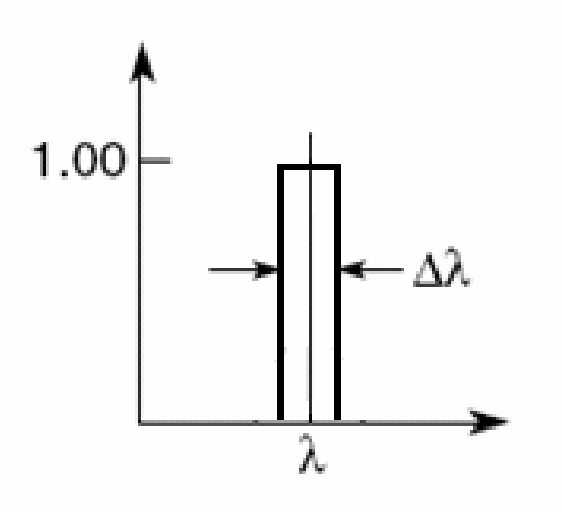

FT

FT^{-1}

Time Domain

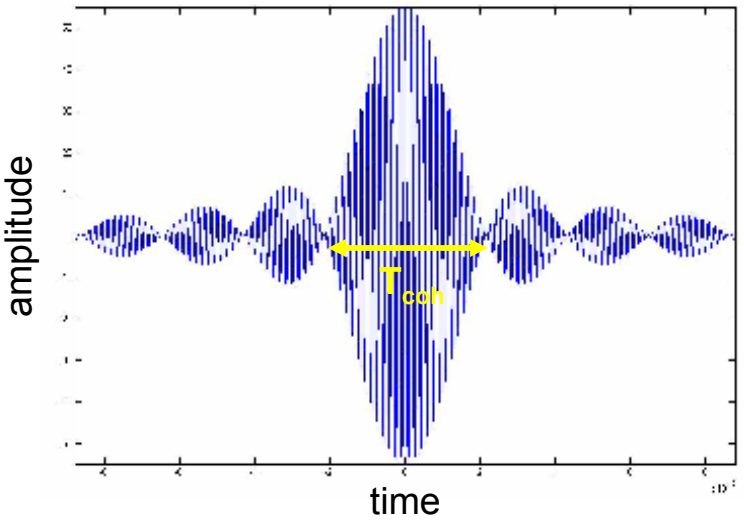

Add all spectral contributions from λ_0–Δλ/2 to λ_0+Δλ/2, assuming equal amplitude *A(l)* for all wavelengths (in actuality closer to Gaussian). Phases φ are constant since the radiation is coming from a single electron.

$$\lambda_0 = 2.4nm \qquad \frac{\Delta\lambda}{\lambda_0} = \frac{1}{55}$$

$$\int_{l=\lambda_0-\frac{\Delta\lambda}{2}}^{\lambda_0+\frac{\Delta\lambda}{2}} A(l)\cos\left(\frac{2\pi c}{l}t+\varphi\right)dl$$

Temporal Coherence and the Michelson Interferometer

Temporal coherence has to do with the ability of the light pulse to form fringes with a delayed version of itself. A common way to do this is to use a Michelson interferometer.

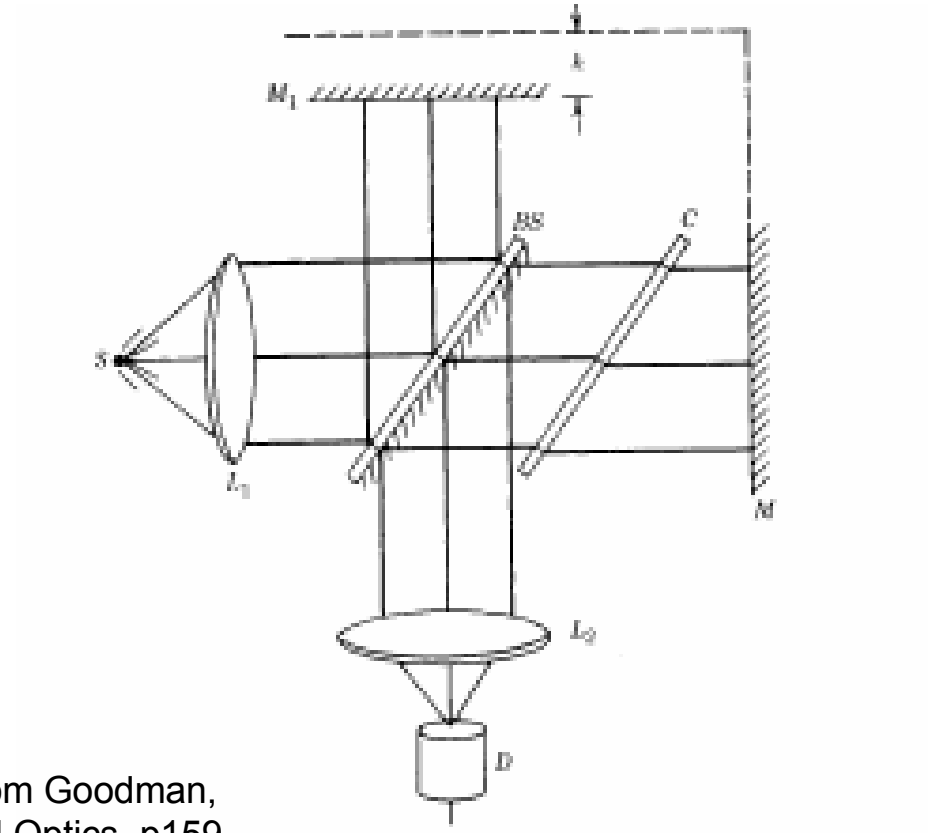

Figure from Goodman, Statistical Optics, p159

Translate one arm of the interferometer to change the optical path difference between the two beams.

Fringes form within the temporal coherence length of the beams.

Measured intensity fringes and temporal coherence time

Time Domain

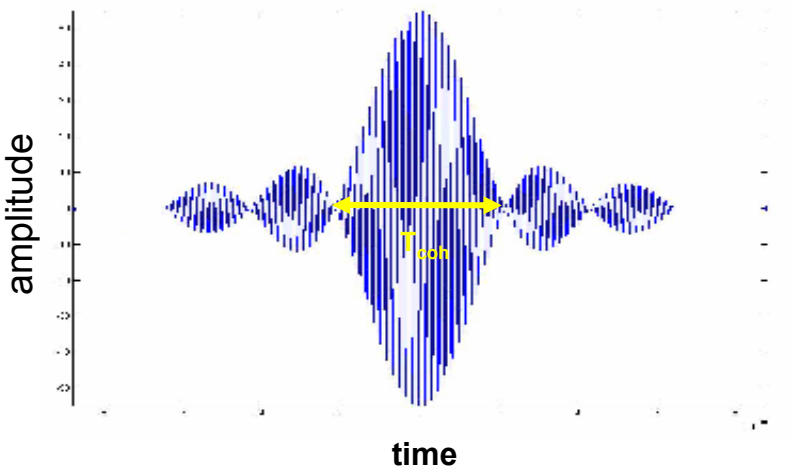

Interfering this beam with a time shifted version of itself (like in the Michelson interferometer) results in the following intensity fringes:

$$L_{coh} \approx \frac{\lambda^2}{\Delta\lambda}$$

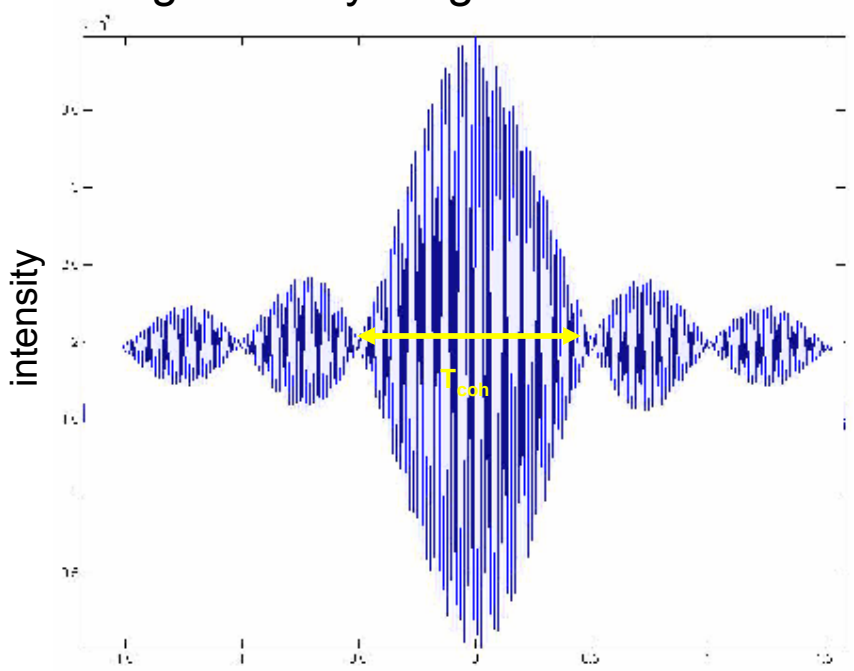

Normalized units of coherence time

Typical Temporal Coherence Lengths

$$L_{coh} \approx \frac{\lambda^2}{\Delta\lambda}$$

Undulator, N = 55, $\Delta\lambda/\lambda$ = 1/55 λ=2.4 nm	$L_{coh} \approx$ 132 nm
Source + Monochrometer, $\Delta\lambda/\lambda$ = 1/3000, λ=2.4 nm	$L_{coh} \approx$ 7.2 μm
Source + Monochrometer, $\Delta\lambda/\lambda$ = 1/10000, λ=2.4 nm	$L_{coh} \approx$ 24 μm
FEL Source (LCLS) $\Delta\lambda/\lambda$ = 1/350, λ=0.25 nm	$L_{coh} \approx$ 86 nm

Spatial Coherence

Spatial Coherence

Ability of spatially separated points in a wavefront to form fringes.

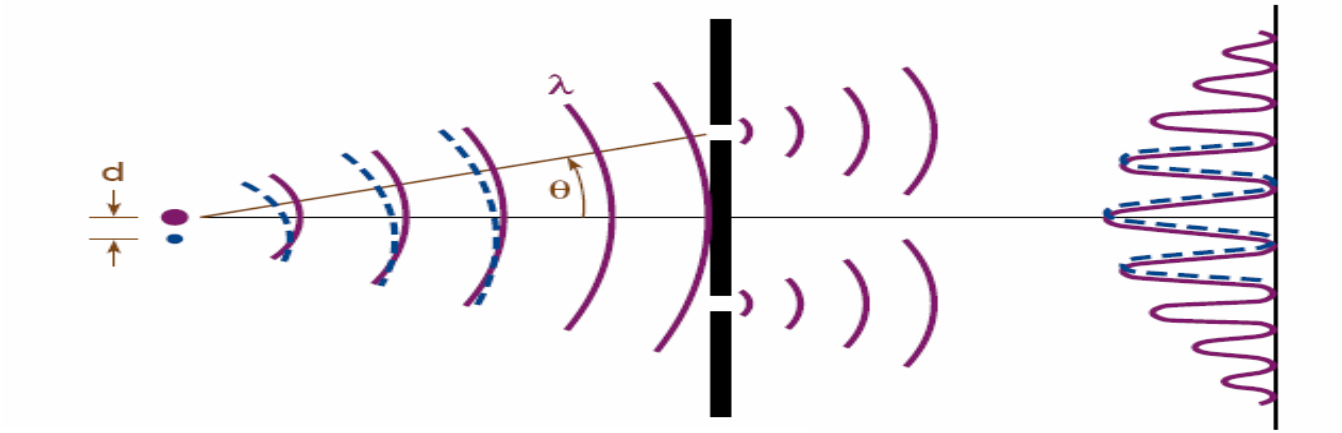

- Associate spatial coherence with a spherical wavefront.
- A spherical wavefront implies a point source.
- How small is a "point source"?

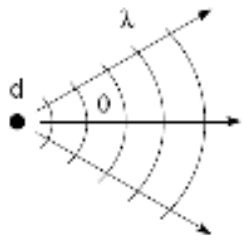

From Heisenberg's Uncertainty Principle ($\Delta x \cdot \Delta p \geq \frac{\hbar}{2}$), the smallest source size "d" you can resolve, with wavelength λ and half angle θ, is

$$d \cdot \theta = \frac{\lambda}{2\pi}$$

$$d \cdot \theta = \frac{\lambda}{2\pi}$$

Obtaining spatial coherence from an undulator using spatial filtering

$$\mathbf{d} \cdot \theta = \frac{\lambda}{2\pi}$$

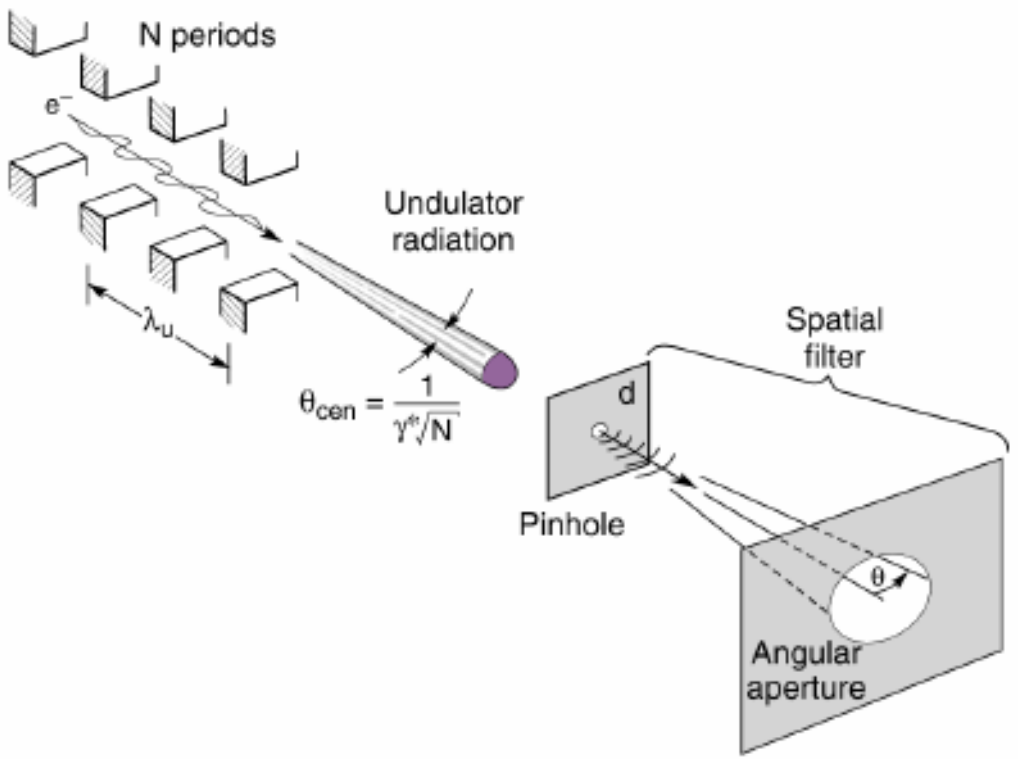

Imaging Applications Using Coherent X-rays

- Lenses
- Holography
- Coherent diffractive imaging

Scattering, Diffraction, and Refraction

(a) Isotropic scattering from a point object

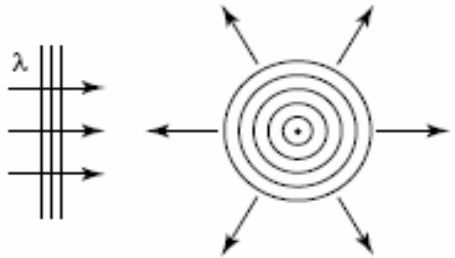

(b) Non-isotropic scattering from a partially ordered system

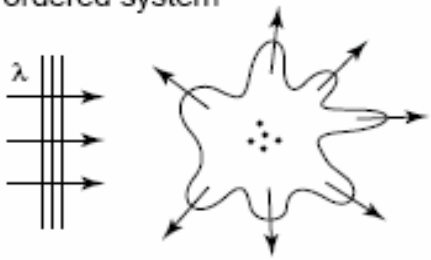

(c) Diffraction by an ordered array of atoms, as in a crystal

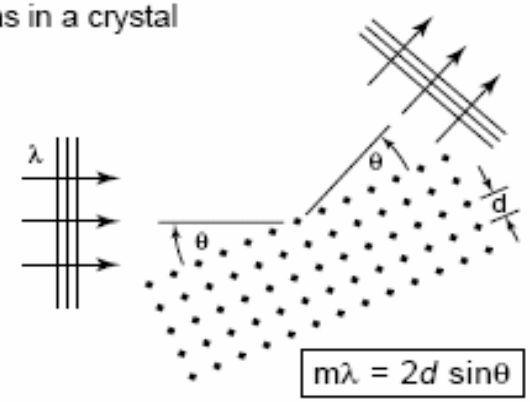

$m\lambda = 2d \sin\theta$

(d) Diffraction from a well-defined geometric structure, such as a pinhole

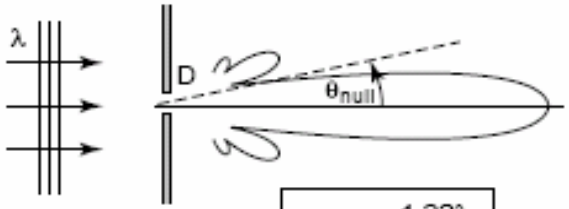

$$\theta_{null} = \frac{1.22\lambda}{d}$$

(e) Refraction at an interface

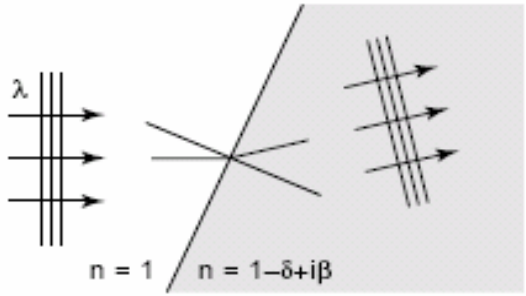

(f) Total external reflection

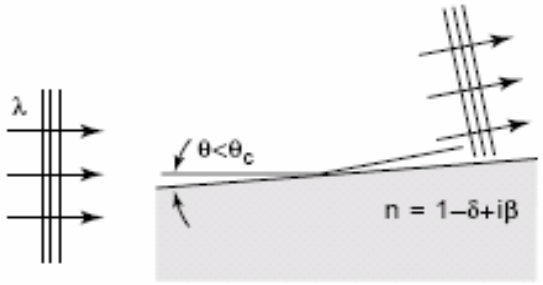

Lens-based imaging

A direct image of the object can be obtained using a lens and CCD.

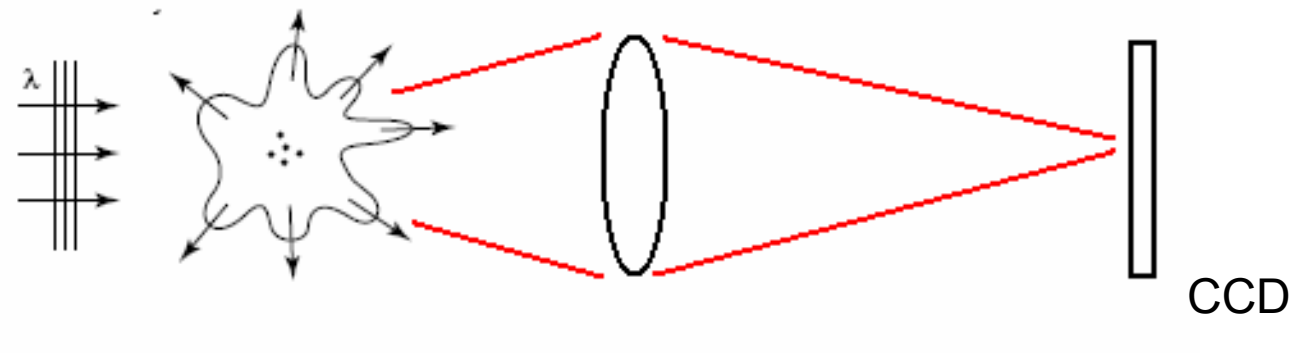

Lens (usually diffractive lenses called zone plates)

Holography

Holography is performed by adding a pinhole near the object and recording the interference pattern from the two. The recorded pattern needs to then be reconstructed (oftentimes something simple, like a Fourier transform) to form an image.

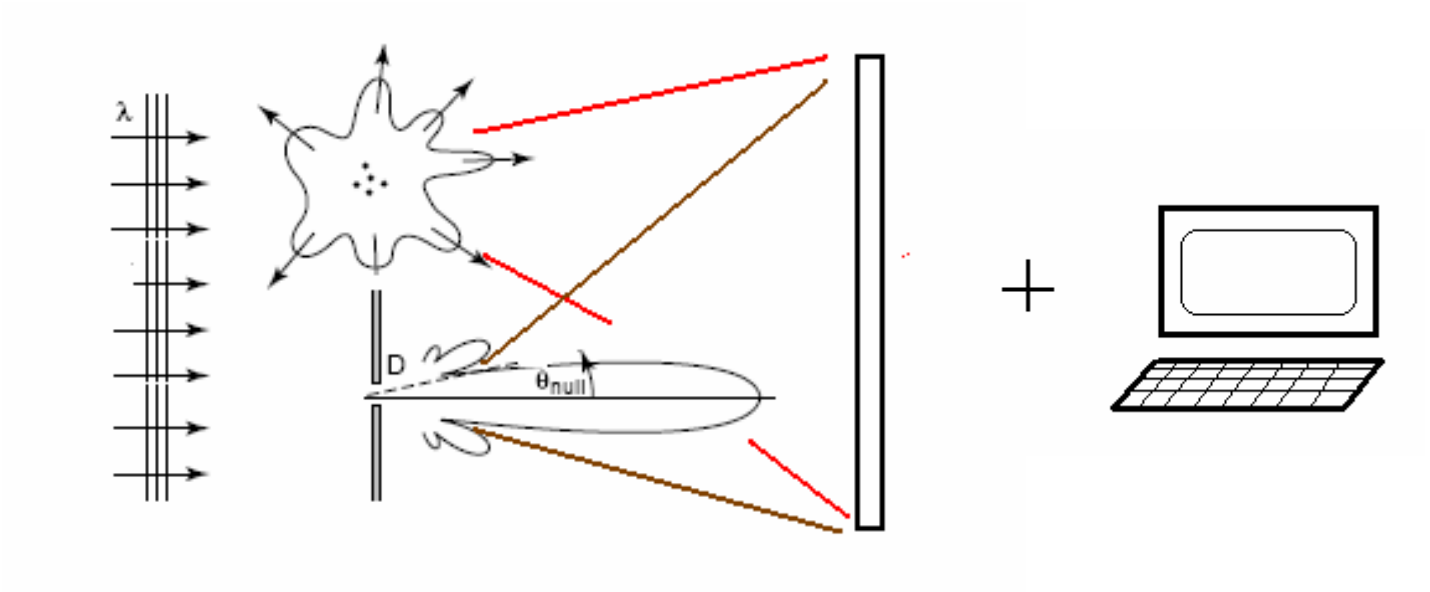

Coherent Diffractive Imaging

Coherent diffractive imaging involves recording an oversampled diffraction pattern directly from an object onto the CCD. The image is then reconstructed using computationally intensive algorithms which recover the phase information.

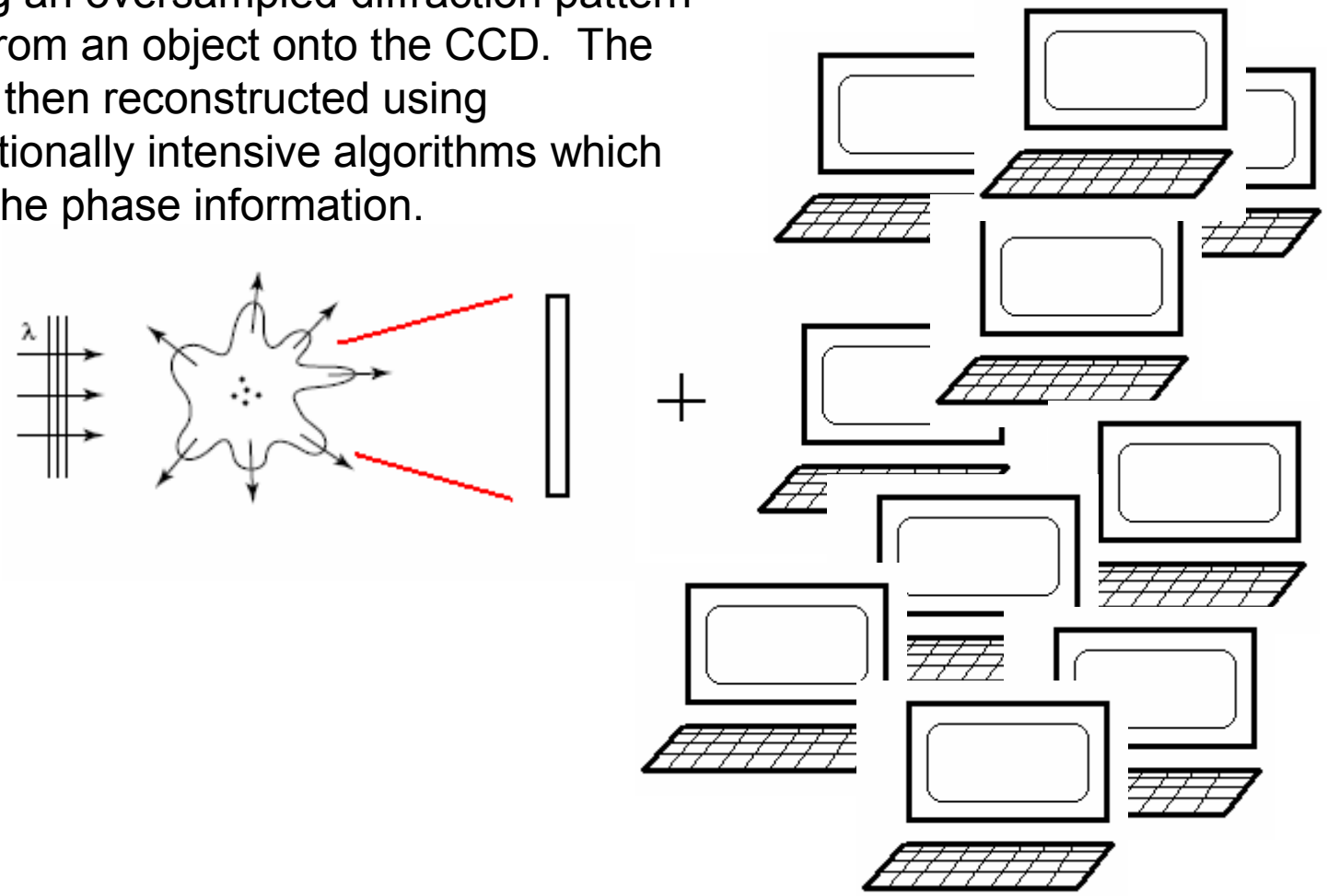

Lens-based imaging

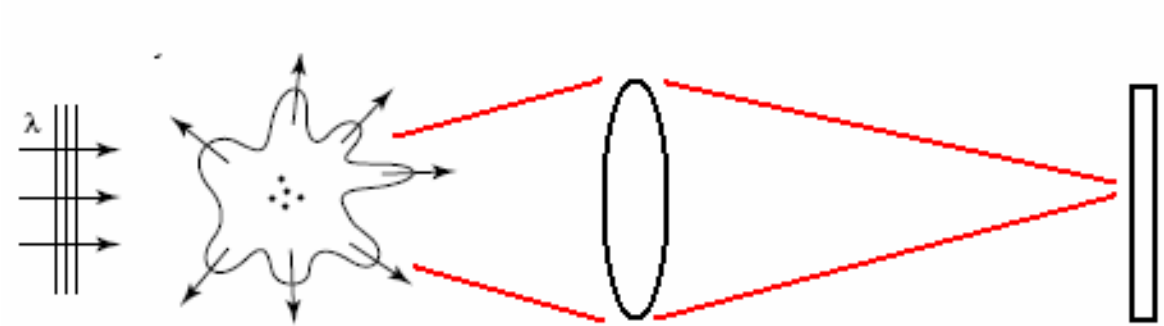

Zone plates lenses are usually used for direct imaging of samples. However, constructing an x-ray microscope using coherent x-rays and a zone plate will lead to imaging with aberrations.

Lens-based imaging with coherent x-rays

Visible light ….

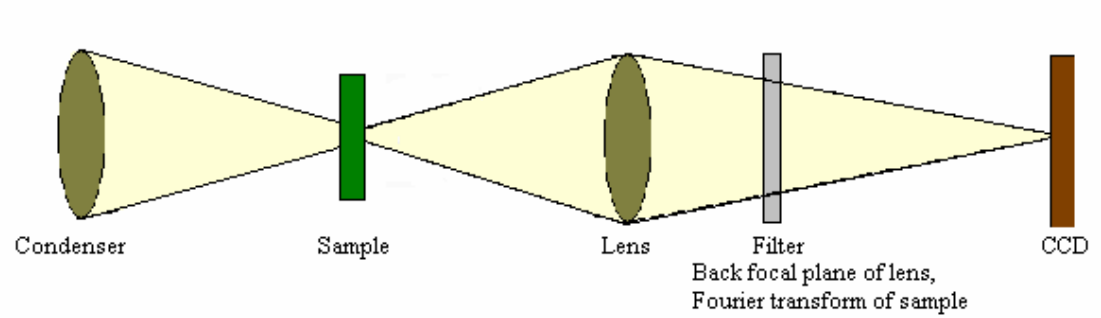

Difficult to make phase plates like this in soft x-ray region due to lack of materials that give appropriate phase shift with adequate transmission and difficult to align.

X-rays ….

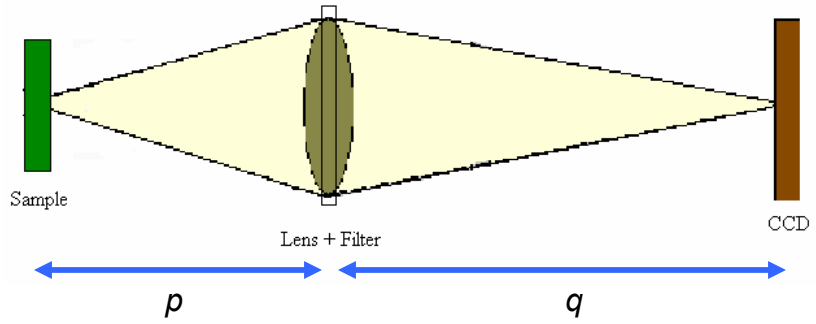

We notice that the Fraunhofer diffraction pattern (which generates a Fourier transform) scales as λ.

$$F = \frac{a^2}{\lambda Z} \qquad \begin{array}{l} Fraunhofer:\ F << 1 \\ Fresnel:\ F >= 1 \end{array}$$

If we make the focal length of the lens greater or equal to the distance Z needed for diffraction in the Fraunhofer regime, AND we have the appropriate imaging geometry, we can combine the lens and filter into one structure and perform imaging.

$$\frac{1}{f} = \frac{1}{p} + \frac{1}{q} \qquad f \geq Z_{Fraunhofer}$$

Spiral phase contrast

Rotating phase

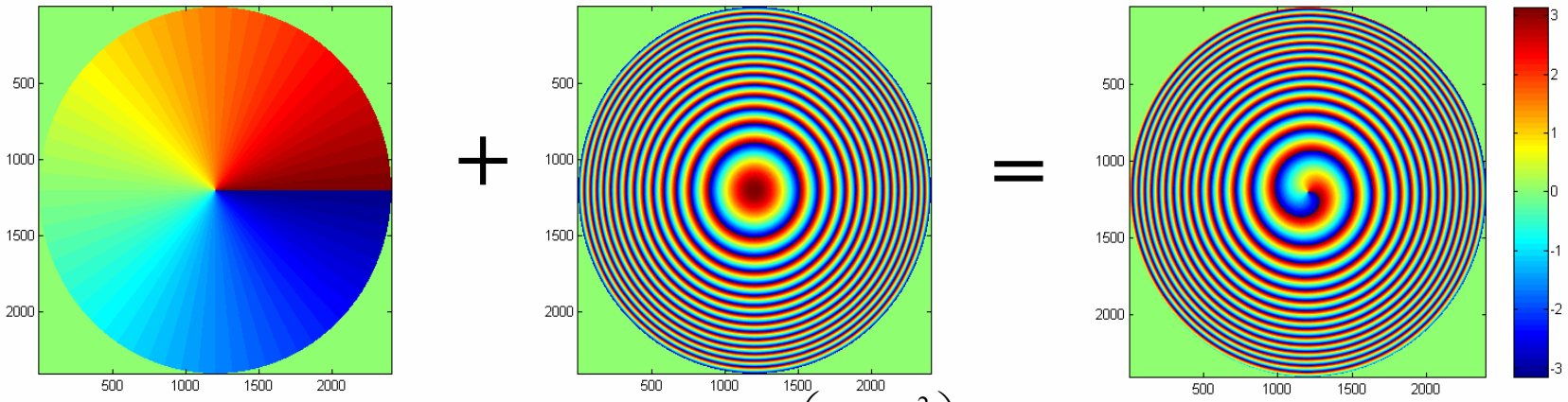

$$Spiralfilter(\rho,\phi) = \exp(im\phi)$$

$$ZP(\rho, f) = \exp\left(\frac{-i\pi\rho^2}{\lambda f}\right)$$

Simulation

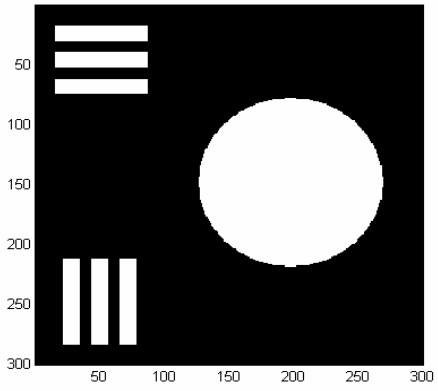

Object

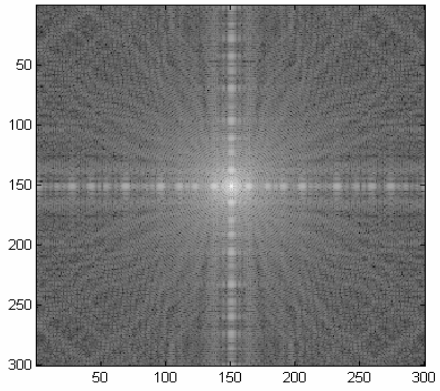

Fourier transform of object

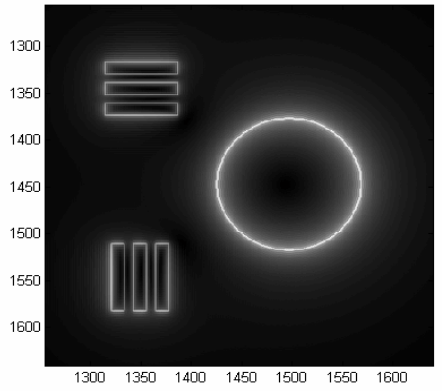

Filtered image

Spiral zone plate

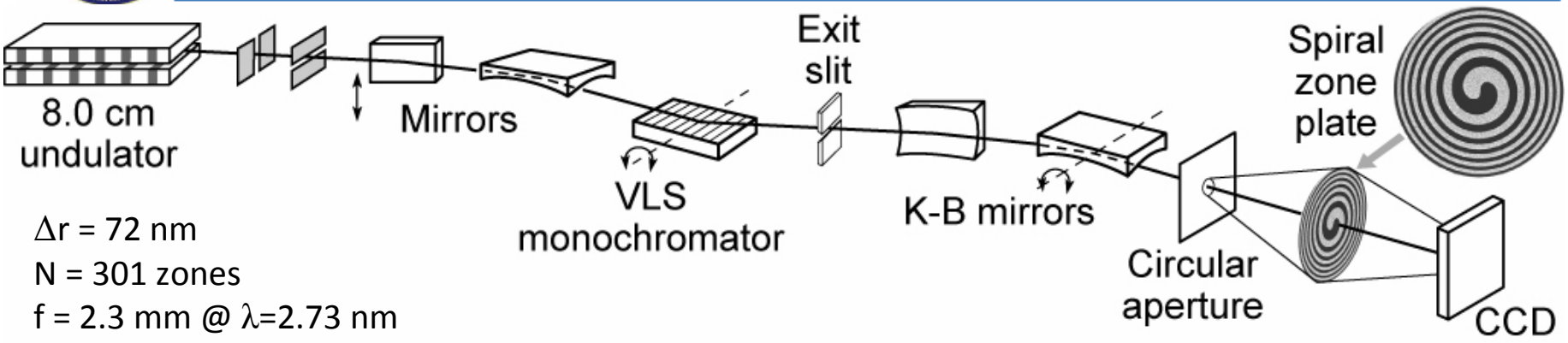

Δr = 72 nm
N = 301 zones
f = 2.3 mm @ λ=2.73 nm

PSF consists of a doughnut-shaped spot with rotating phase

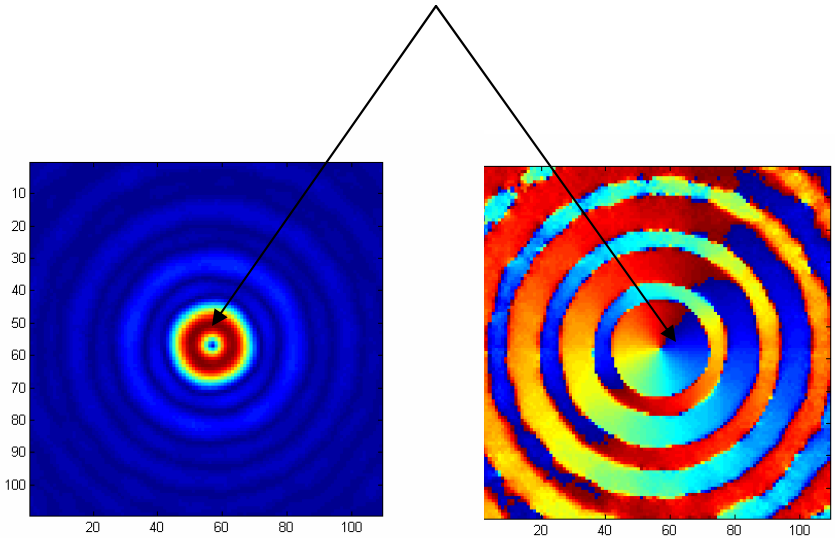

Magnitude PSF

Phase PSF

SZP charge 1

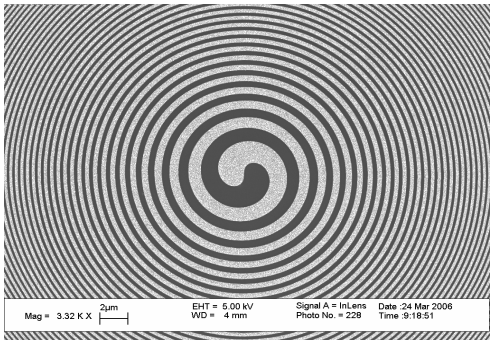

SZP charge 2

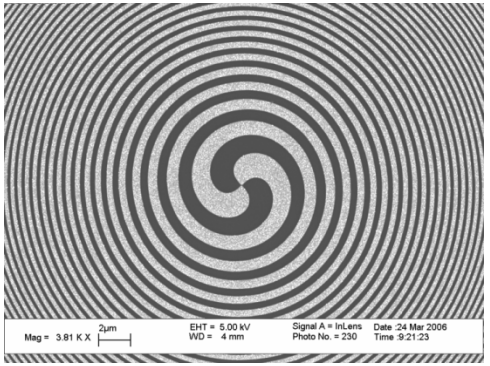

Edge enhanced imaging using a spiral zone plate

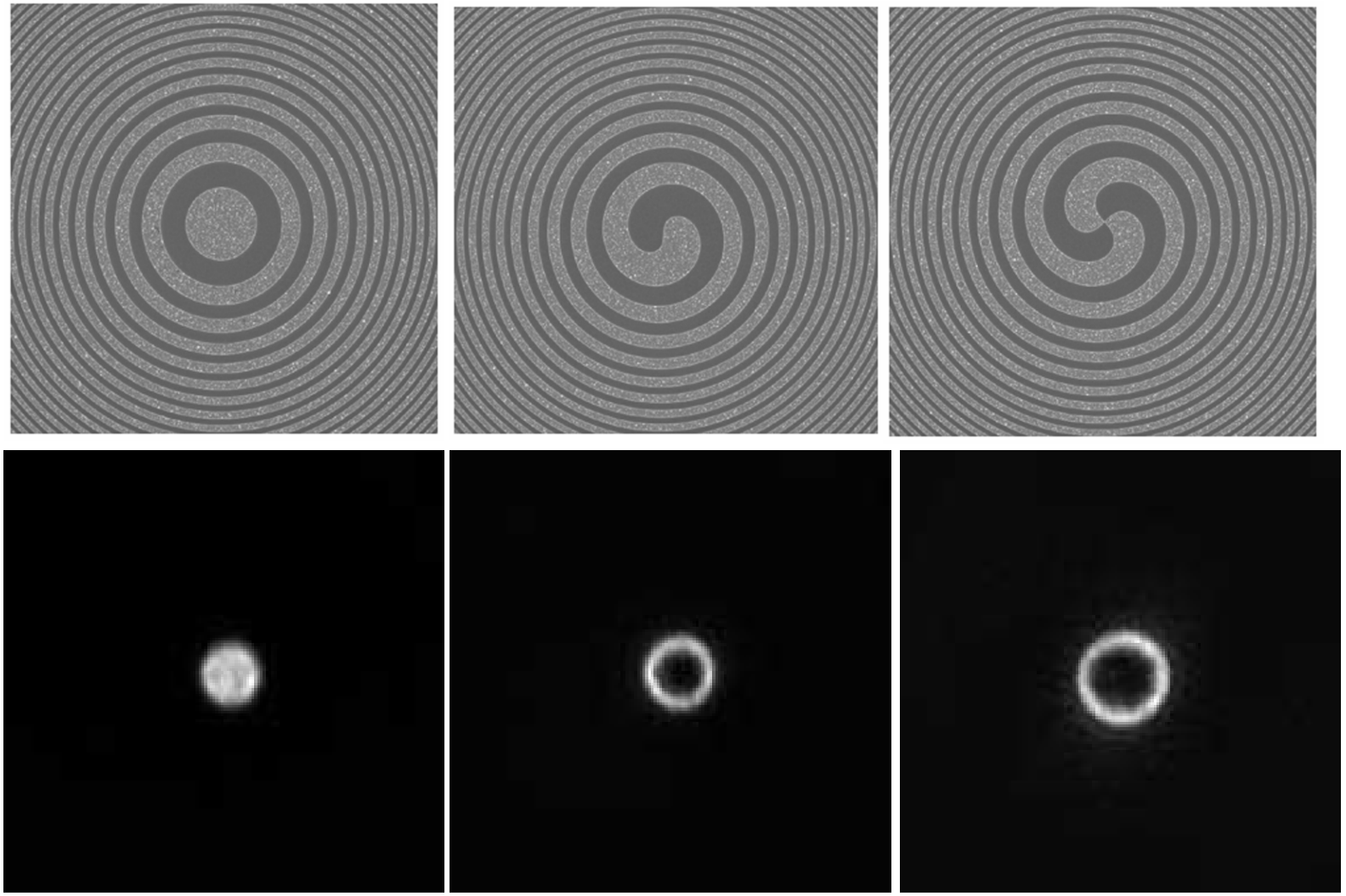

1 micron pinhole at λ =2.73 nm

Holography

Holography is performed by adding a pinhole near the object and recording the interference pattern from the two. The recorded pattern needs to then be reconstructed (oftentimes something simple, like a Fourier transform) to form an image.

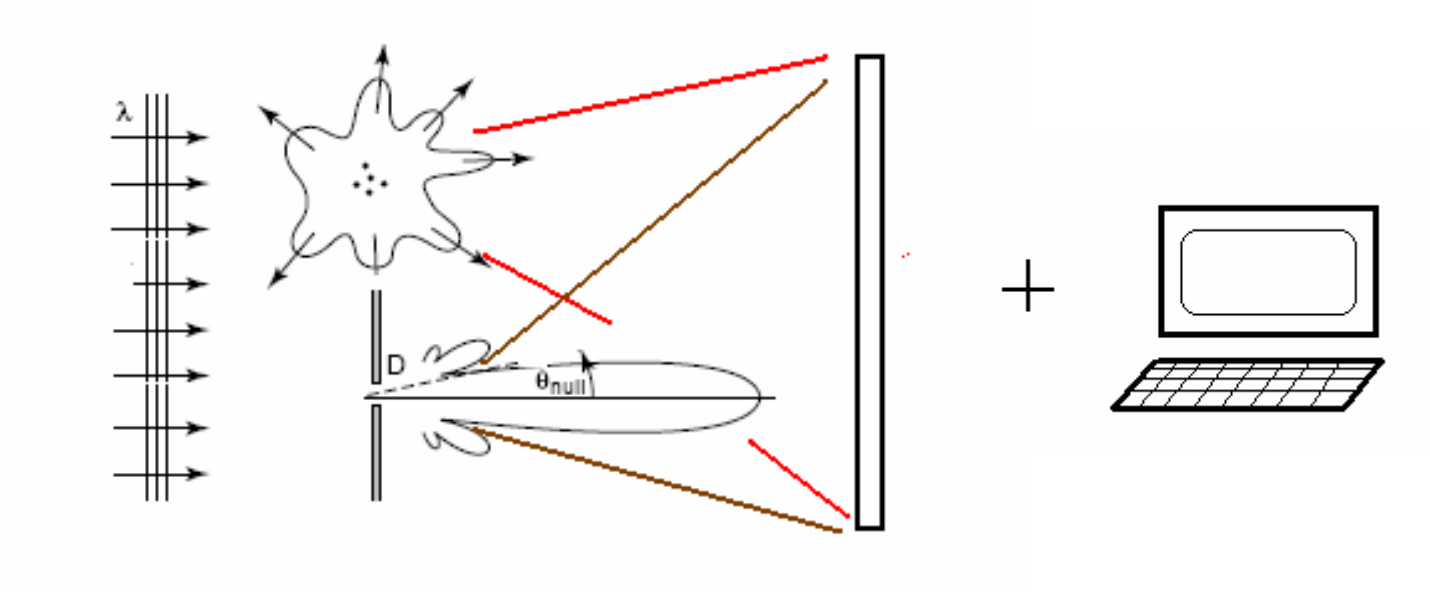

Fourier transform holography

Single pinhole reference holography

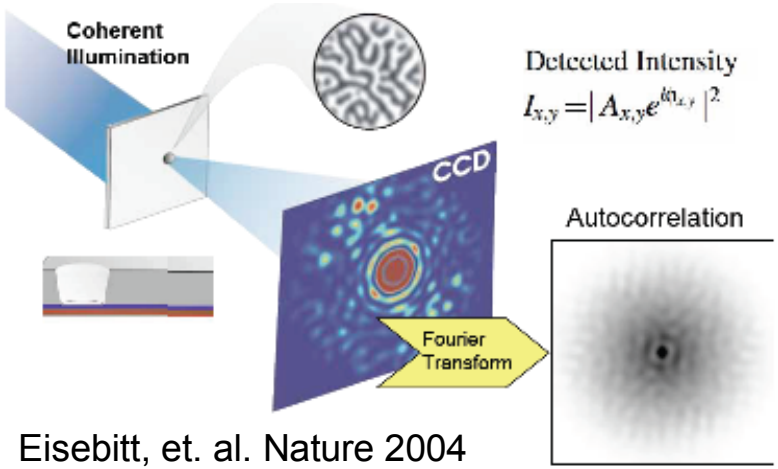

Eisebitt, et. al. Nature 2004

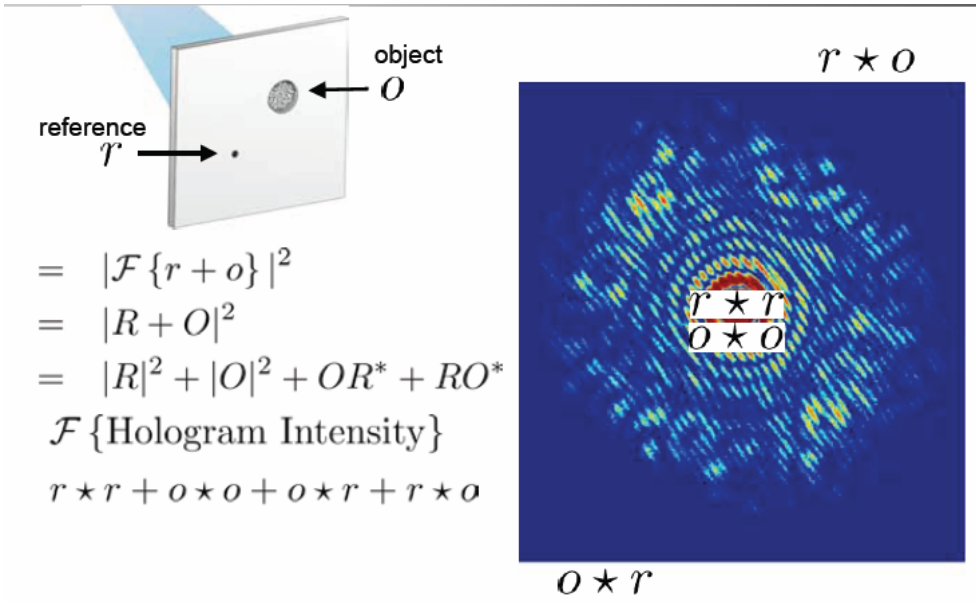

- The squared magnitude of the complex autocorrelation is shown.
- Sub-Images ready for extraction.
- Five sub-images are essentially identical and have the same orientation
- They can be aligned for averaging by cross correlation.

W. F. Schlotter, R. Rick, K. Chen, et. al., Appl. Phys. Lett. 89 (2006)

Multiple reference holography improves signal to noise and resolution.

Slides from Bill Schlotter, currently at DESY

Signal to noise limits resolution in Fourier transform holography

Fourier transform holography simulation using the same number of photons

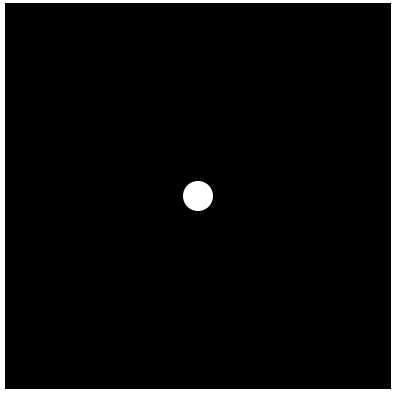

With a single pinhole reference

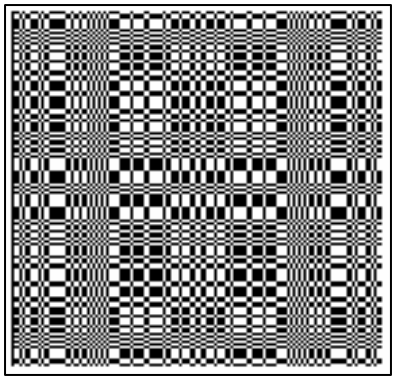

With a URA (uniformly redundant array) coded aperture reference

Low resolution or noise

High resolution & low noise

Courtesy of Stefano Marchesini

Massively parallel holography

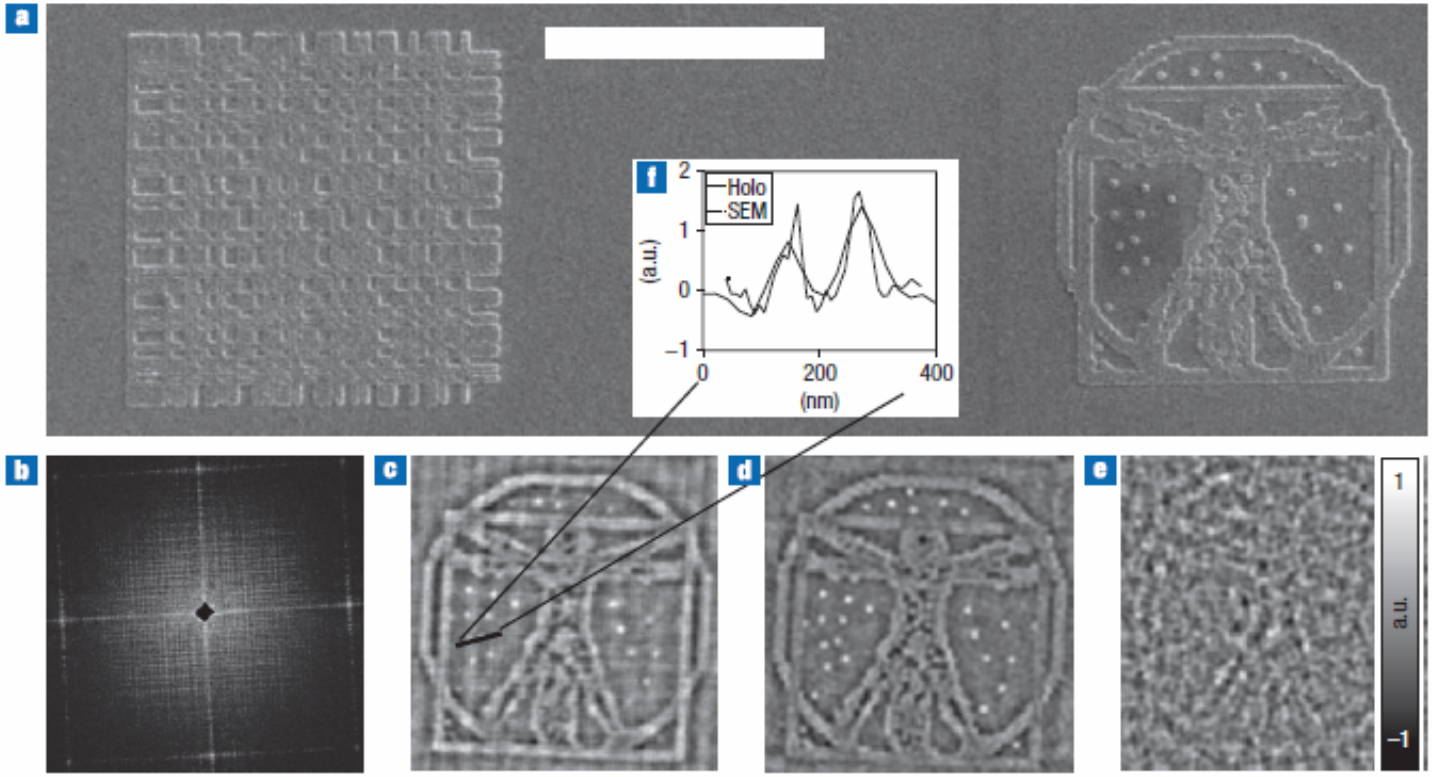

Figure 2 Massively parallel holography at high resolutions. **a**, A lithographic test sample imaged by scanning electron microscopy (SEM) next to a 30-nm-thick twin-prime 71 × 73 array with 44-nm square gold scattering elements. The scale bar is 2 μm. **b**, The diffraction pattern collected at the ALS ($\lambda = 2.3$ nm, 1×10^6 photons in 5-s exposure, 200 mm from the sample). **c**, The real part of the reconstructed hologram. **d**, The simulation with 1×10^6 photons. The grey scale represents the real part of the hologram. **e**, A simulation with the same number of photons, but a single reference pinhole. **f**, Line through the two dots indicated in **c**.

Q9

S. Marchesini , et. al. Nature Photonics 2008

Coherent Diffractive Imaging

Coherent diffractive imaging involves recording an oversampled diffraction pattern directly from an object onto the CCD. The image is then reconstructed using computationally intensive algorithms which recover the phase information.

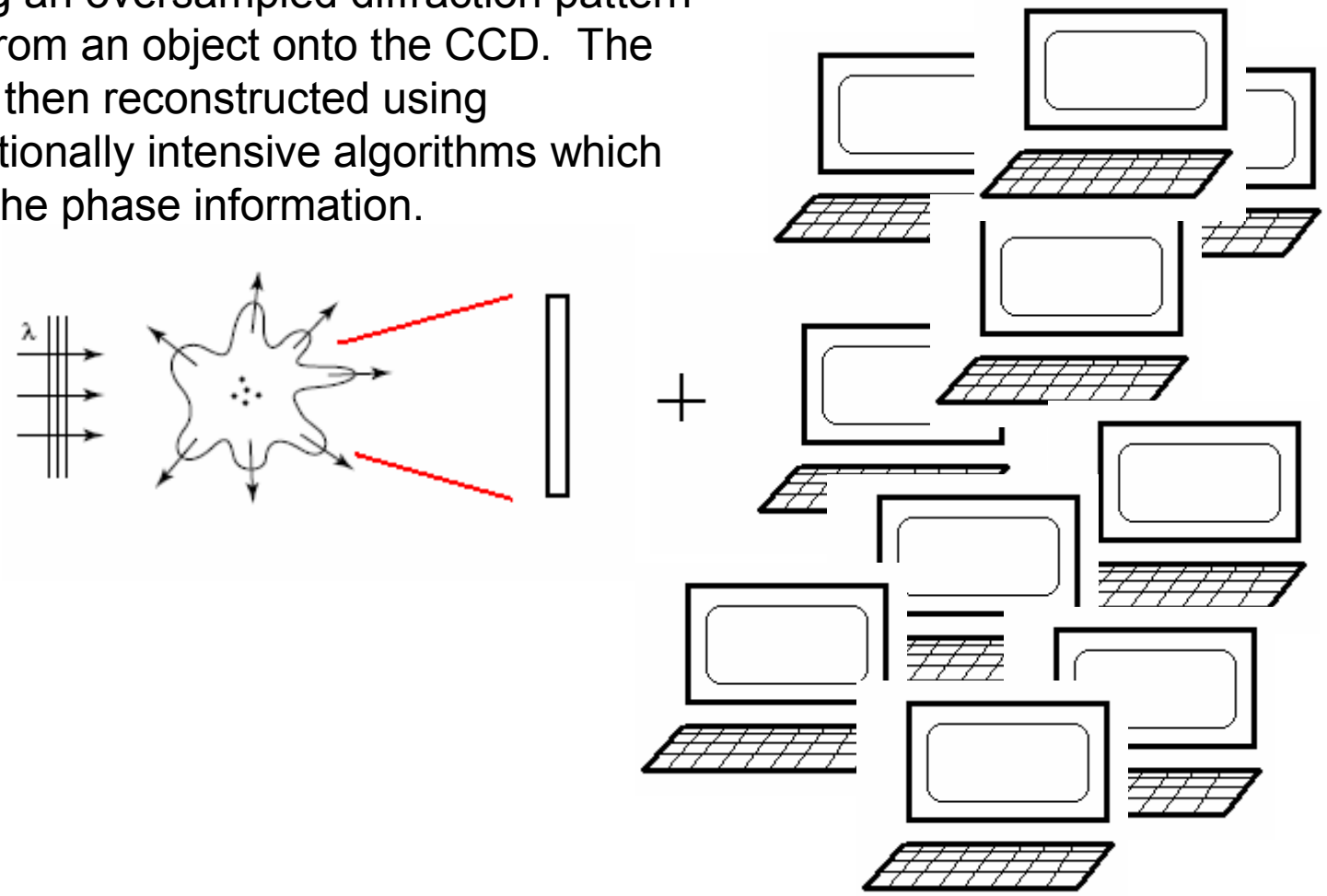

Coherent Diffraction Imaging

1. Record diffraction pattern from non-crystalline sample illuminated by coherent x-rays

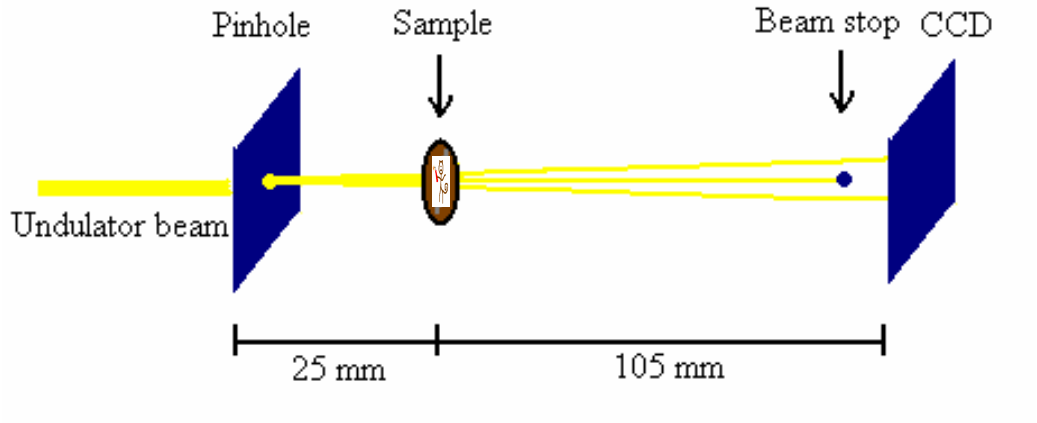

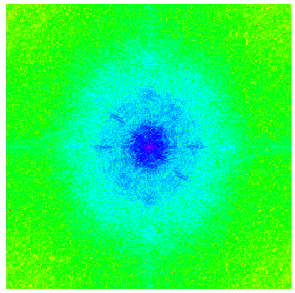

Diffraction Pattern (Magnitude)

2. Phase-retrieval

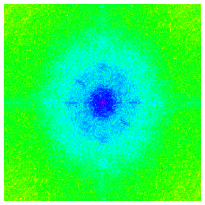

Magnitude

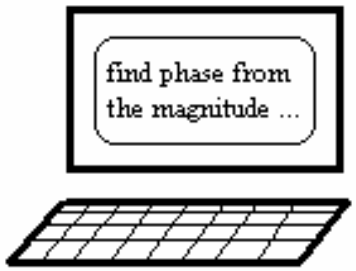

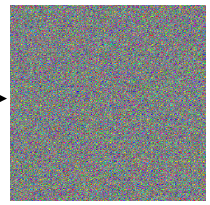

Phase

3. Fourier inversion

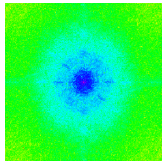

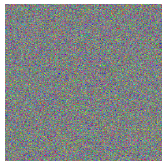

$\mathcal{F}^{-1}\{\ \}$

CDI: Obtaining a diffraction pattern

Oversampling (Sayre, Bates)

Sampling at a frequency greater than that of the Bragg frequency

$$O = \frac{r_{no-density}}{r_{electron-density}}$$

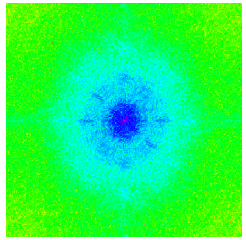

Not oversampled

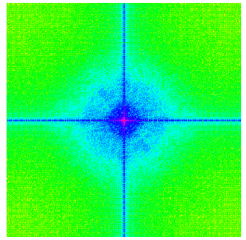

O=1

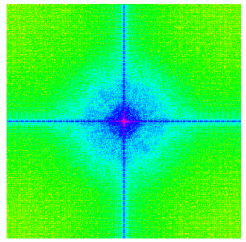

O=2

Coherence requirements

$$\theta \leq \frac{\lambda}{2Oa}$$

$$\frac{\lambda}{\Delta\lambda} \geq \frac{Oa}{d}$$

a is object size, d is desired resolution

Resolution

- Determined by signal to noise in diffraction pattern
- Limited by source and/or radiation damage

CDI: Phase Retrieval and Fourier Inversion

Step 2: Phase information recovered using phase-retrieval algorithms

Hybrid Input Output Algorithm (Fienup)

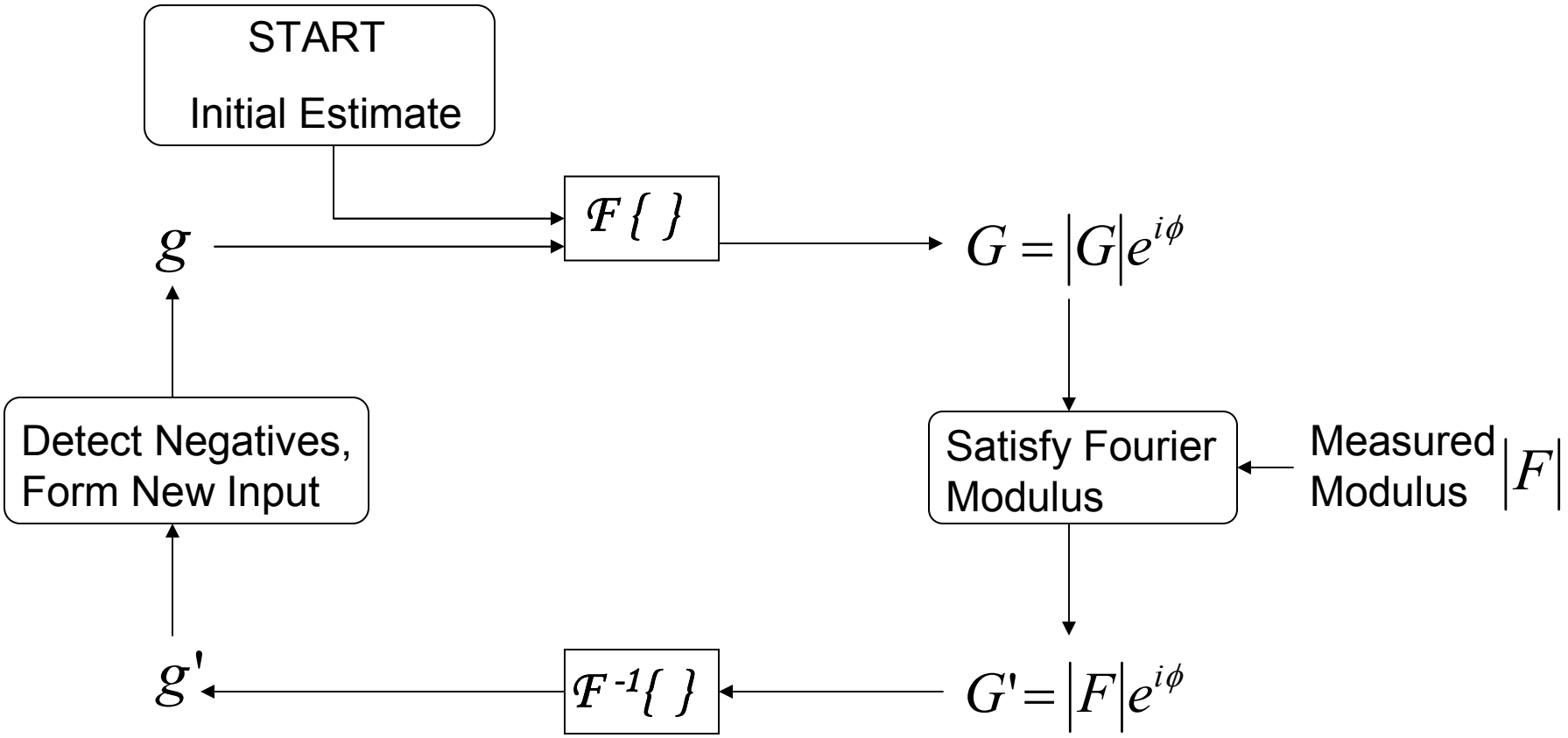

Step 3: Object recovered by Fourier inversion

CDI Examples

Synchrotron CDI with 3D distribution of Au particles (E 750 eV, res 10 nm)

Chapman, et. al. JOSA A 2006

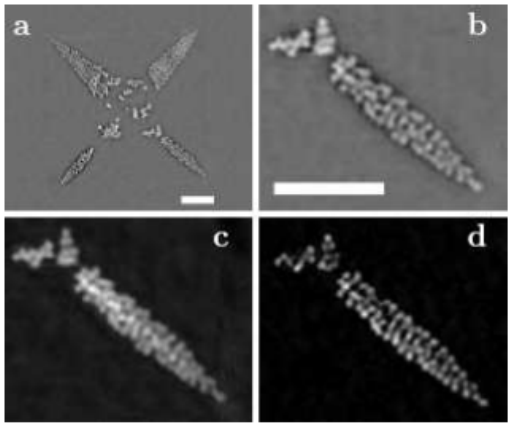

Fig. 8. Infinite depth of focus projection images, for the object orientation $\phi = 0°$. (a) Reconstruction from a 2D central section interpolated from the 3D diffraction dataset. The reconstruction was performed without a positivity constraint, $E_S^2 = 0.167$. (b) Enlargement of the lower right arm of (a). (c) [and also Fig. 2 (c)] Reconstruction from the 2D central section, using a positivity constraint, $E_S^2 = 0.072$. (d) Projected image formed by integrating the full 3D reconstructed image, $E_S^2 = 0.113$. The scalebars are 500 nm.

Synchrotron CDI with dried yeast cell (E 750 eV, res 30 nm)

Shapiro, et. al. PRL 2005

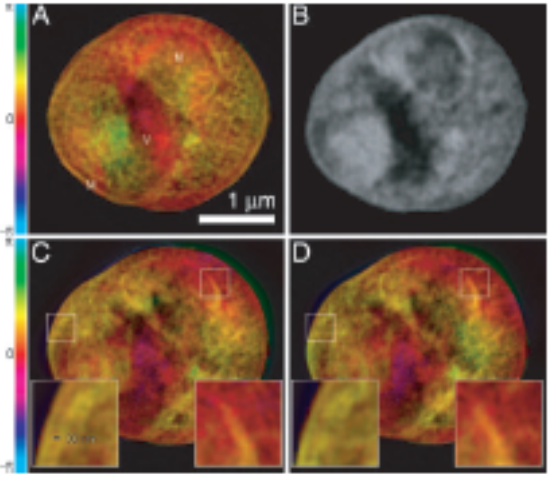

Fig. 3. Images of a freeze-dried yeast cell. *A* was obtained by phasing the diffraction data in Fig. 1, whereas *C* and *D* were obtained from reconstructions of two separate, slightly lower exposure data sets acquired with the cell tilted by 3° (*C*) and 4° (*D*) relative to *A* (Movie 2, which is published as supporting information on the PNAS web site, displays reconstructed images at 1° intervals over a 7° range). *Insets* in *C* and *D* show ~30-nm fine features at the cell and nuclear membrane regions that are reproduced consistently in these separate recordings and reconstructions, even though these 2D reconstructions are projections along the beam axis with some blurring as a result of defocus. The renderings of the complex-valued reconstructions use brightness to represent magnitude and hue to represent phase (the color scale indicates reconstructed phase values). *A* is labeled according to a provisional identification of the nucleus (N), a storage vacuole (V), and the cell membrane (M). *B* shows a National Synchrotron Light Source X1A2 STXM (27) image taken of the same cell using 540-eV x-rays and a zone plate with an estimated Rayleigh resolution of 42 nm; this image shows absorption effects only, so it is shown in grayscale. The STXM image is shown here for comparison purposes only; it was taken at a different photon energy and in a different contrast mode (incoherent brightfield) than applies to the reconstructed diffraction data. The information contained in the STXM image was not used in any way in obtaining the diffraction reconstruction.

Synchrotron CDI with Aerogel particle (E 750 eV, res 15 nm)

Barty, et. al. PRL 2008

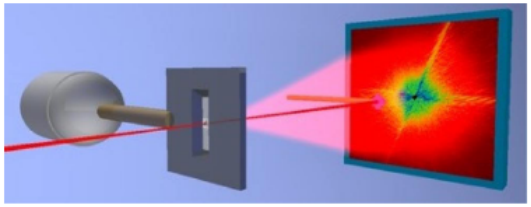

FIG. 1 (color online). Diffraction imaging layout. Coherent x rays ($\lambda = 1.65$ nm) illuminate [26,27] the sample mounted on a 50 nm thick Si_2N_3 membrane window. Diffraction patterns at various sample orientations ($+69°$ to $-64°$ in $1 \pm 0.1°$ increments) are measured using a CCD camera (20 μm pixel size, 1300×1340 pixels, 165 mm downstream). A beamstop blocks the direct beam and multiple exposure times are summed to expand the CCD dynamic range.

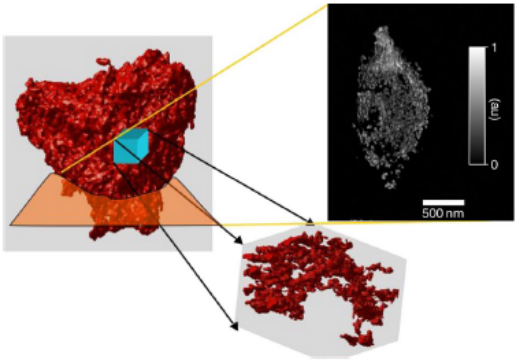

FIG. 3 (color online). Section and isosurface rendering of a 500 nm cube from the interior of the 3D volume. The foam structure shows globular nodes that are interconnected by thin beamlike struts. Approximately 85% of the total mass is associated with the nodes, and there is no evidence of a significant fraction of dangling fragments.

CDI: Examples

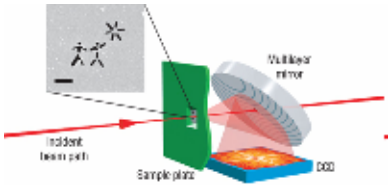

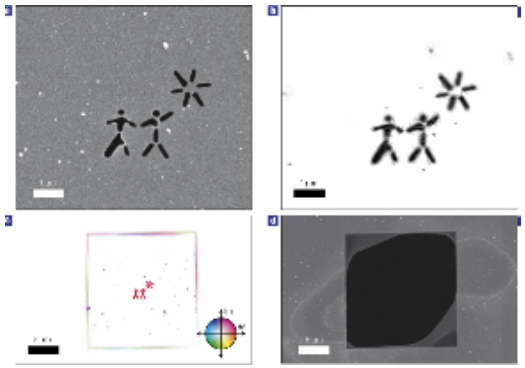

FELCDI with artificially fabricated pattern (E 38 eV, res 32 nm)

Chapman, et. al. Nat. Phys 2006

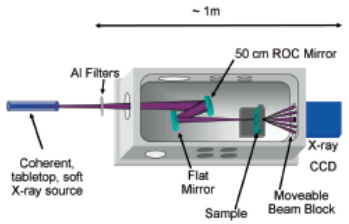

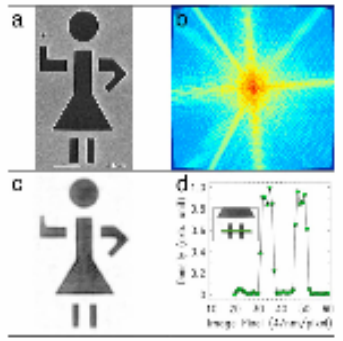

HHG CDI with artificially fabricated pattern (E 43 eV, res 45 nm)

Sandberg, et. al. PNAS 2008

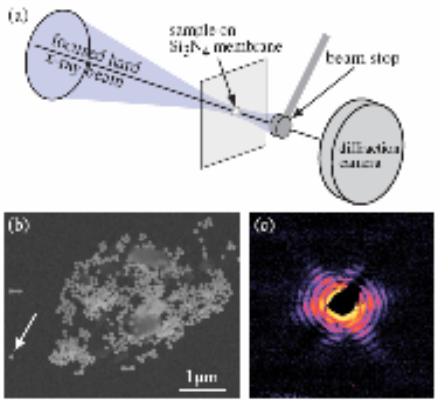

FIG. 1 (color online). (a) Schematic sketch of the coherent diffraction imaging setup with nanofocused illumination. (b) Scanning electron micrograph of gold particles (diameter ≈ 100 nm) deposited on a Si_3N_4 membrane. (c) Diffraction pattern (logarithmic scale) recorded of the single gold particle pointed to by the arrow in (b) and illuminated by a hard x-ray beam with lateral dimensions of about 100 × 100 nm^2. The maximal momentum transfer, both in horizontal and vertical direction, is $q = 1.55\ nm^{-1}$.

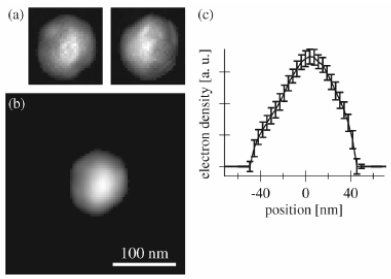

FIG. 2. (a) Two individual reconstructions of the gold particle using the HIO algorithm, a left- and a right-handed one. To obtain the average particle shape from a series of reconstructions with random initial phases, the right-handed reconstructions were inverted and averaged together with the left-handed ones. (b) Reconstructed projected electron density of the gold nanoparticle shown in Fig. 1(b) after averaging the series of reconstructions. (c) Horizontal section through the center of the particle shown in (b). The error bars indicate rms variations in the density for the series of independent reconstructions.

Synchrotron CDI with Au particle (E 15 keV, res 5 nm)

Schroer, et. al. PRL 2008

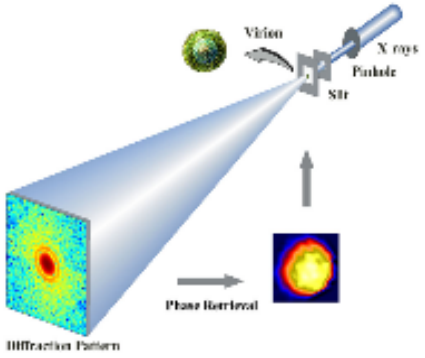

FIG. 1 (color online). Schematic layout of the x-ray diffraction microscope. A 20-μm pinhole was used to define the incident x-ray beam. The virion specimen was positioned at a distance of 1 m from the pinhole. A silicon guard slit with beveled edges was used to eliminate the parasitic scattering from the pinhole. The oversampled diffraction pattern, recorded on a liquid-nitrogen cooled CCD camera, was directly inverted to a high-contrast image using an iterative algorithm.

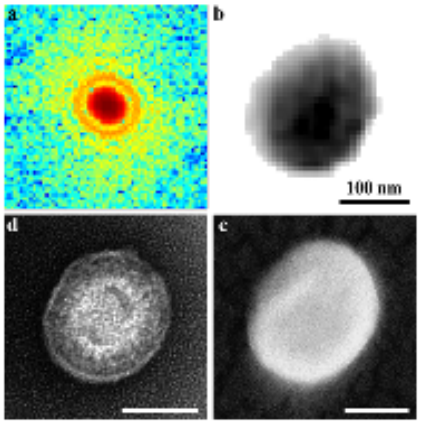

FIG. 2 (color online). X-ray diffraction imaging of single herpesvirus virions. (a) X-ray diffraction pattern obtained from a single, unstained virion. (b) High-contrast image reconstructed from (a) where the background and the surroundings of the virion were completely removed. (c) SEM image of the same virion. (d) Negative stain TEM image of a similar herpesvirus virion.

Synchrotron CDI with single unstained virus (E 5 keV, res 22 nm)

Song, et. al. PRL 2008

Holography and CDI can be used together in imaging

Hologram: Provides more constraints in the reconstruction algorithm, helping it converge more rapidly

CDI: Extends the resolution of the holographic image

Keyhole coherent diffractive imaging

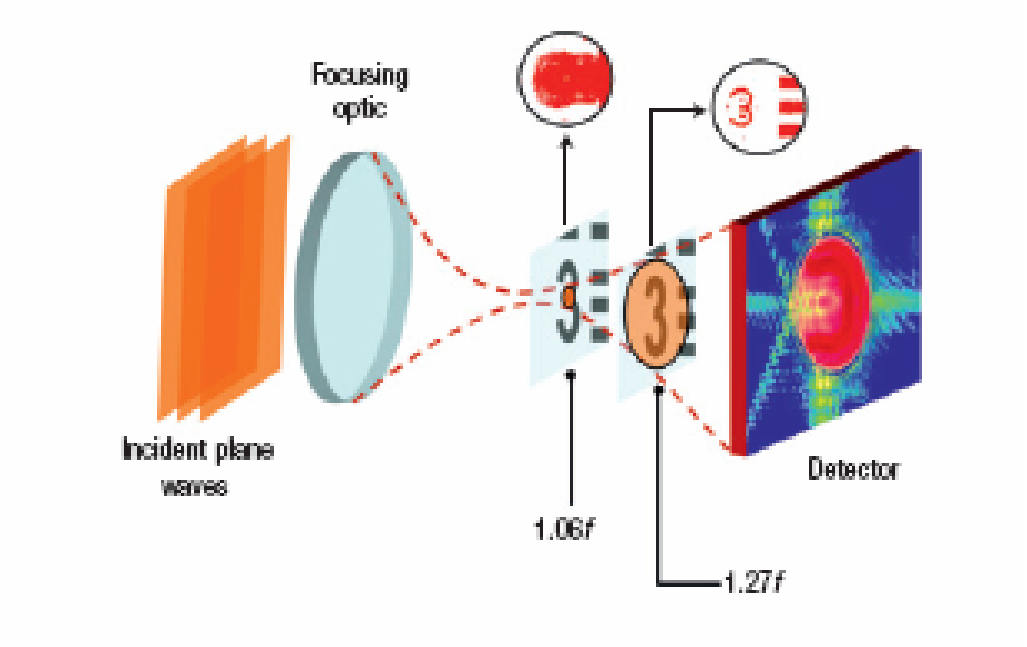

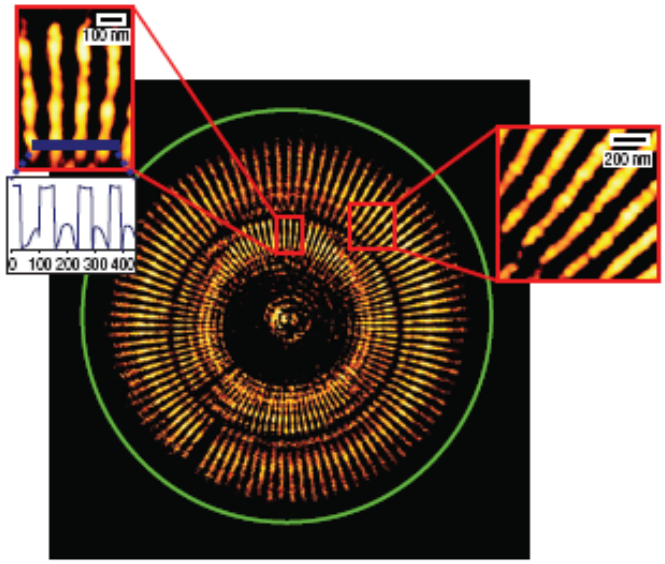

- Limited coherence area of beam would limit sample size since it requires a finite support .

- This technique overcomes this:

  - Support formed using zone plate focus

  - Extended sample can be used and scanned with zone plate focus

B. Abbey, K. Nugent, G. Williams, et. al. Nature Physics 2008

Zone plate focusing for CDI at FLASH FEL

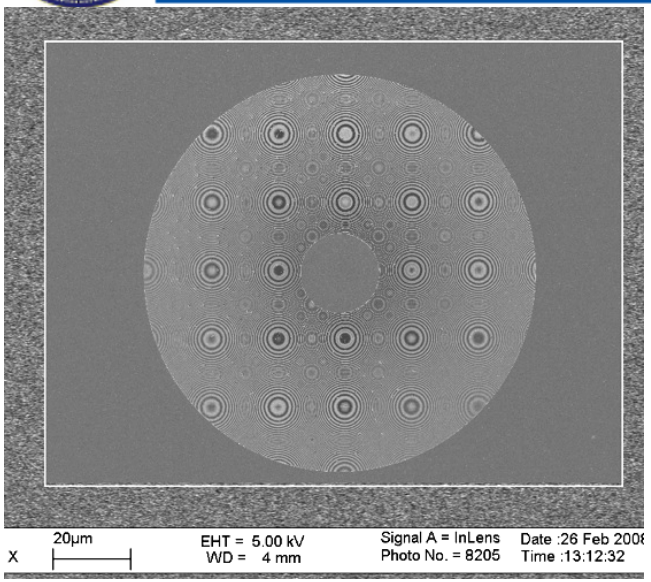

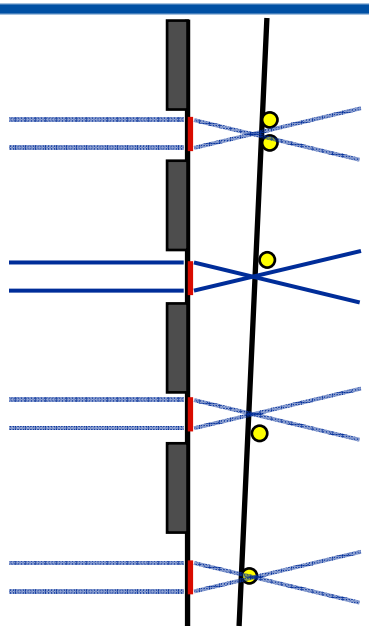

Array of ~200 zone plates
35 nm outermost zone width
100 micron diameter
0.5 mm focus at 7 nm wavelength

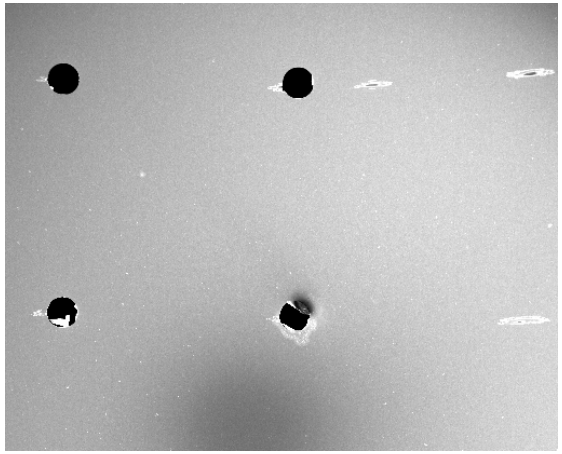

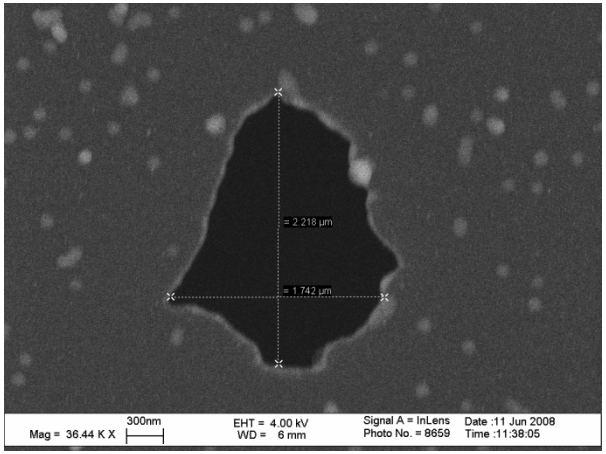

The zone plate should achieve about 2 orders of magnitude greater intensity than the beamline optic

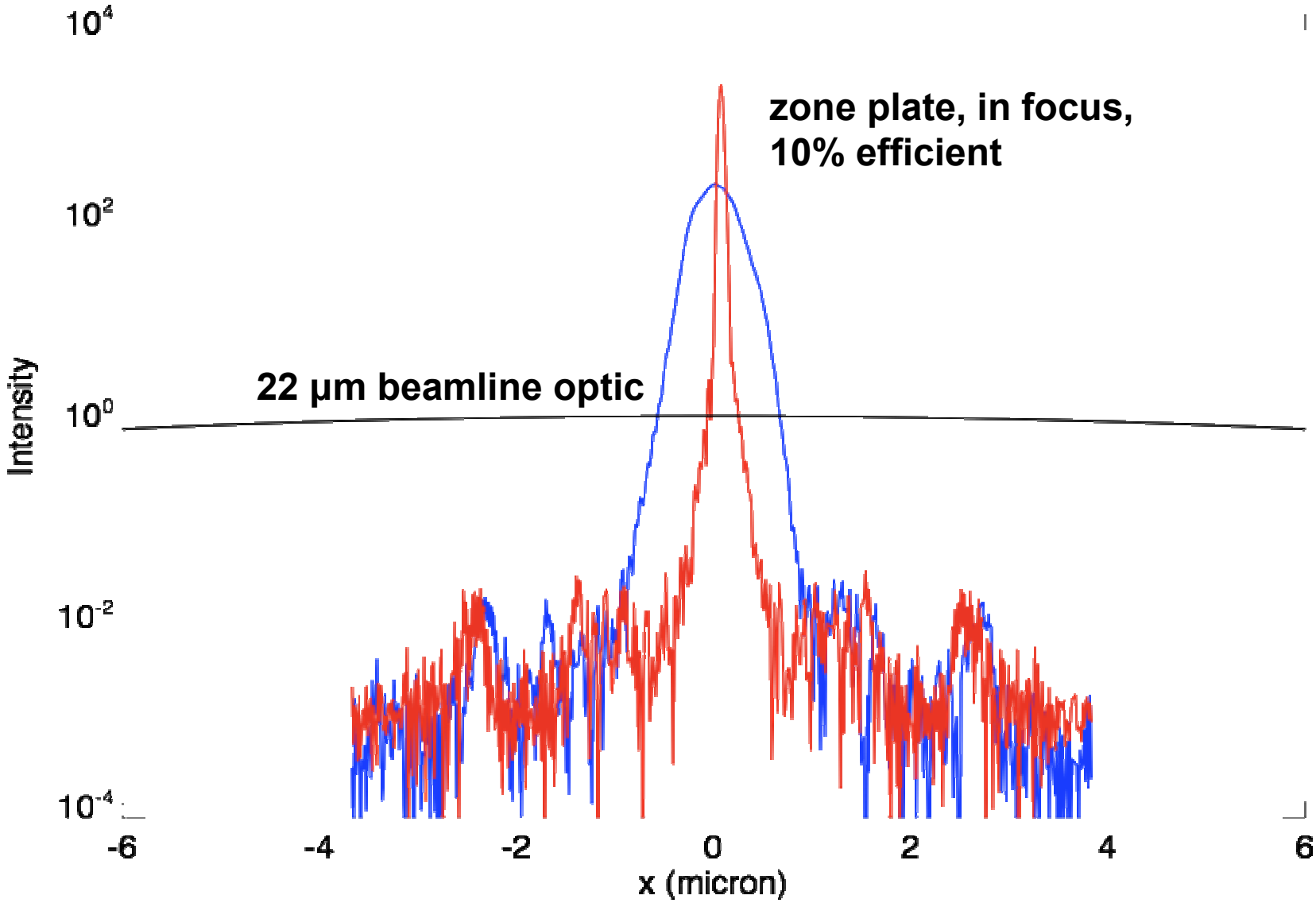

Courtesy of Henry Chapman

Comparison of Techniques

Lens-based

- Direct imaging
- Resolution limit determined by smallest feature size in lens
- Use with coherent light often involves operating in an off-axis configuration

Holography

- Indirect imaging, but reconstruction not terribly complicated
- Resolution limit determined by smallest feature size in reference and signal to noise (last item can be overcome by using multiple references or massively parallel coded aperture refrences)

CDI

- Indirect imaging, and reconstruction is complicated
- Resolution limit determined by detector resolution, as well as signal to noise

Use of these techniques in conjunction with one another ….

FLASH FEL
http://flash.desy.de/

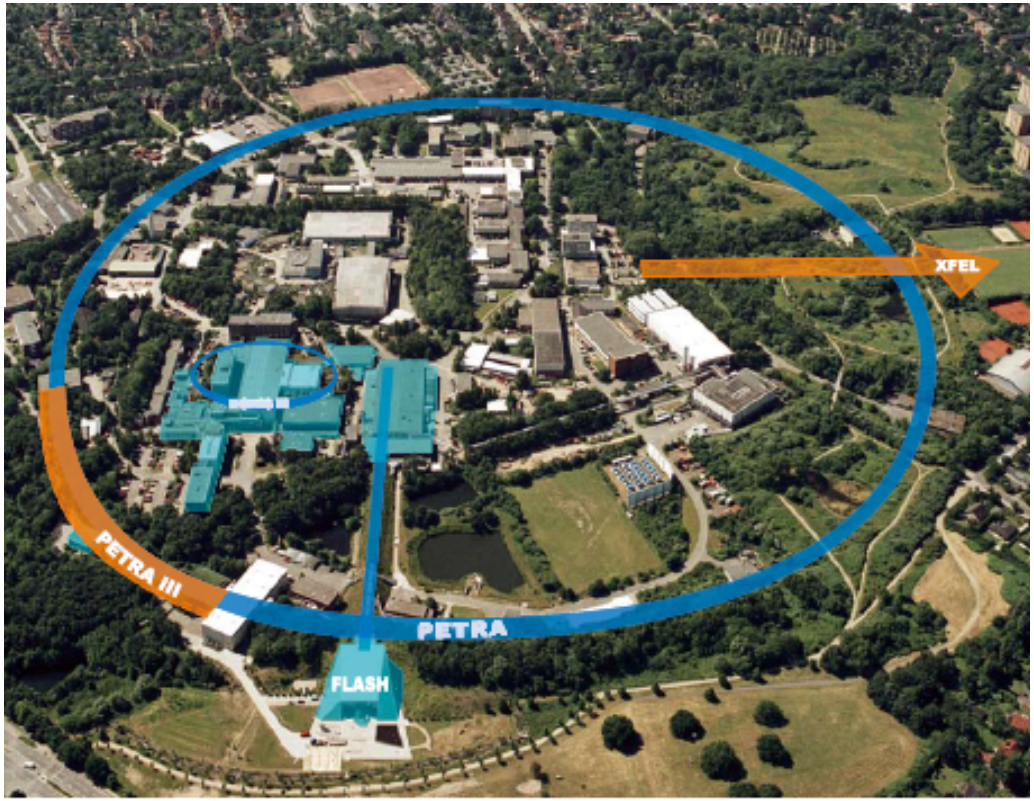

FLASH

The latest addition to the range of light sources on offer at DESY is the FLASH free-electron laser, which commenced user operation in summer 2005. FLASH will remain unrivalled worldwide until 2009. The 260-metre-long facility is the world's first light source to deliver laser radiation in the X-ray range with high peak brilliance and ultra-short light pulses – and it does so at the shortest wavelengths ever achieved with a free-electron laser. Initial usage of this facility has already resulted in some spectacular new experiments, and the scientific interest is correspondingly intense. FLASH offers a total of five experimental stations, where different instruments can be set up as required. At the same time, the operation of FLASH generates important knowledge for the forthcoming XFEL X-ray laser and similar light sources worldwide.

XFEL – the European X-ray laser

An absolute highlight in the genuine sense of the word is the forthcoming European X-ray free-electron laser XFEL, which will generate extremely intense, ultra-short pulses of laser light in the X-ray range at wavelengths substantially shorter than even the light generated by FLASH. The XFEL will therefore open up a whole new realm of highly promising research opportunities for almost all the natural sciences. The 3.4-kilometre-long facility extends from DESY in Hamburg to the Schleswig-Holstein town of Schenefeld in the Pinneberg district, where the research campus will be located, comprising an experimental hall and space for ten experimental stations. There is also room here to build, if required, a second experimental complex with ten additional stations. The XFEL was approved in principle in February 2003 and is to be realized as an independent European project. At the beginning of June 2007 the German research ministry gave the go-ahead for construction of an initial version with six experimental stations, to be funded by Germany and international partners. The start of commissioning is scheduled for 2013.

FLASH IMAGE.

„FLASH, what a picture!“

“FLASH, what a picture!” was the cover story of the 12 December 2006 issue of *nature physics*. What so excited the *nature* editors was an image produced at the new FLASH facility, featuring two tiny stick figures beneath an equally tiny sun. This might sound anything but sensational. However, this “flash diffraction image” was a significant breakthrough in experimental methods. In one of the very first experiments at FLASH, the researchers had succeeded in using a single laser flash to obtain a detailed diffraction image of the sample, which was only a few micrometres in size, before it was destroyed by the intense light. And there was another reason for their excitement: The small stick figures and their sun were engraved in a thin membrane. This meant that the sample was not crystalline, yet a single laser pulse was sufficient to obtain a meaningful image.

This first application of the flash diffractive imaging method demonstrates that it should soon be possible to use single ultra-short, extremely intense laser pulses to record images of nanoparticles, or even of individual large macromolecules. The new method therefore holds the promise of extraordinary capabilities for studying the dynamics of nanoparticles and the structure of large biomolecules, viruses, or cells, without the need to first subject the sample to a complex crystallization process, as is the case in conventional structural analysis using X-rays.

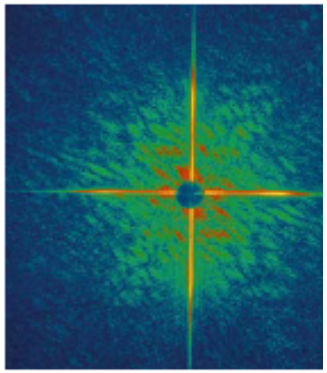

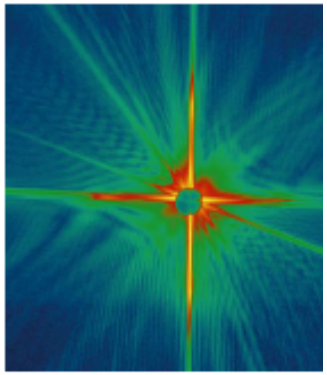

Top: Diffraction image of a sample, recorded with a single ultra-short, extremely intense and coherent laser pulse from the FLASH free-electron laser
Bottom: Diffraction image of the same sample after its destruction by the first laser pulse

Imaging methods are often limited by the fact that the
tion used to create the image also damages the samp
that insufficiently strong signals are recorded by the d
tors. One way to avoid this is to crystallize the molecu
be studied, so that many of them can be examined si
neously. But there is a problem with this method. In m
cases it is very difficult to crystallize the material. Esp
in the life sciences this is a significant limitation, beca
molecules are especially difficult or even impossible t
crystallize.

However, there is a way to circumvent the problem. R
searchers need to record the image before the sampl
destroyed by the radiation, preferably by using a light
of such intensity that a single flash is sufficient to deli
required signal. This approach also has the advantage
crystallization is necessary. Flash diffractive imaging c
requires a single molecular complex to be irradiated w
single ultra-short, very intense X-ray laser pulse. Usin

number of these diffraction images, it then becomes possible to determine the spatial arrangement of the atoms. Thanks to FLASH, the international team of researchers has now been able to prove that this method actually works.

The flash diffractive imaging principle heralds a revolution in structural research in the natural sciences – particularly when images with very high temporal and spatial resolution are required. Since the new imaging method requires no lenses, it can be extended to provide resolution on an atomic scale as soon as X-ray lasers with even shorter wavelengths become available. As a result, the FLASH experiment also backs up the high hopes for revolutionary new experimental capabilities that are being placed in the future generation of hard X-ray free-electron lasers, such as the Linac Coherent Light Source LCLS at Stanford (USA) or the European XFEL facility in Hamburg.

> Deutsches Elektronen-Synchrotron DESY, Germany
> Spiller X-ray Optics, USA
> Stanford Synchrotron Radiation Laboratory, Stanford Linear Accelerator Center SLAC, USA
> Technical University of Berlin, Germany
> University of California, Davis, USA
> University of California, Lawrence Livermore National Laboratory, USA
> University of Uppsala, Sweden

The experiment in detail

To create the diffraction image, the researchers illuminated a thin membrane into which a three-micrometre-wide pattern – of two cowboys under a sun – had been cut, with a FLASH light pulse of 32 nanometres wavelength and only 25 femtoseconds duration. The energy of the laser pulse heated the sample to about 60 000 degrees Celsius, causing it to vaporize. But the team succeeded in recording a diffraction pattern before the sample was destroyed. The image derived from the diffraction pattern by special mathematical methods showed no discernible sign of radiation damage, and it was possible to reconstruct the test object to the maximum possible resolution. Damage to the sample did not occur until after the ultra-short laser pulse had passed through it.

> micrometre: millionth of a metre
> nanometre: billionth of a metre
> femtosecond: quadrillionth of a second

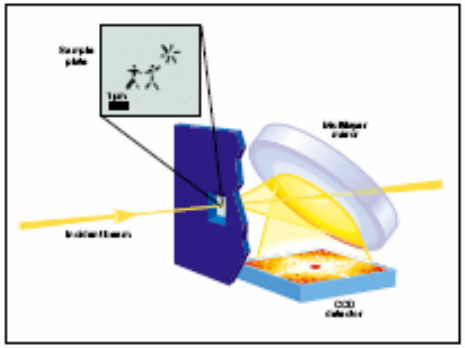

Schematic representation of the flash diffractive imaging experiment at the FLASH free-electron laser

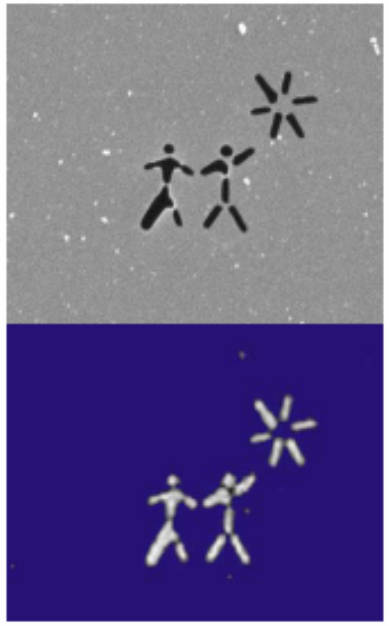

Top: The sample under the scanning electron microscope – two stick figures under a sun, cut into a membrane with a thickness of just a few nanometres
Bottom: Reconstruction of the pattern from the recorded diffraction image

Workshop report
http://repositories.cdlib.org/lbnl/LBNL-1034E/

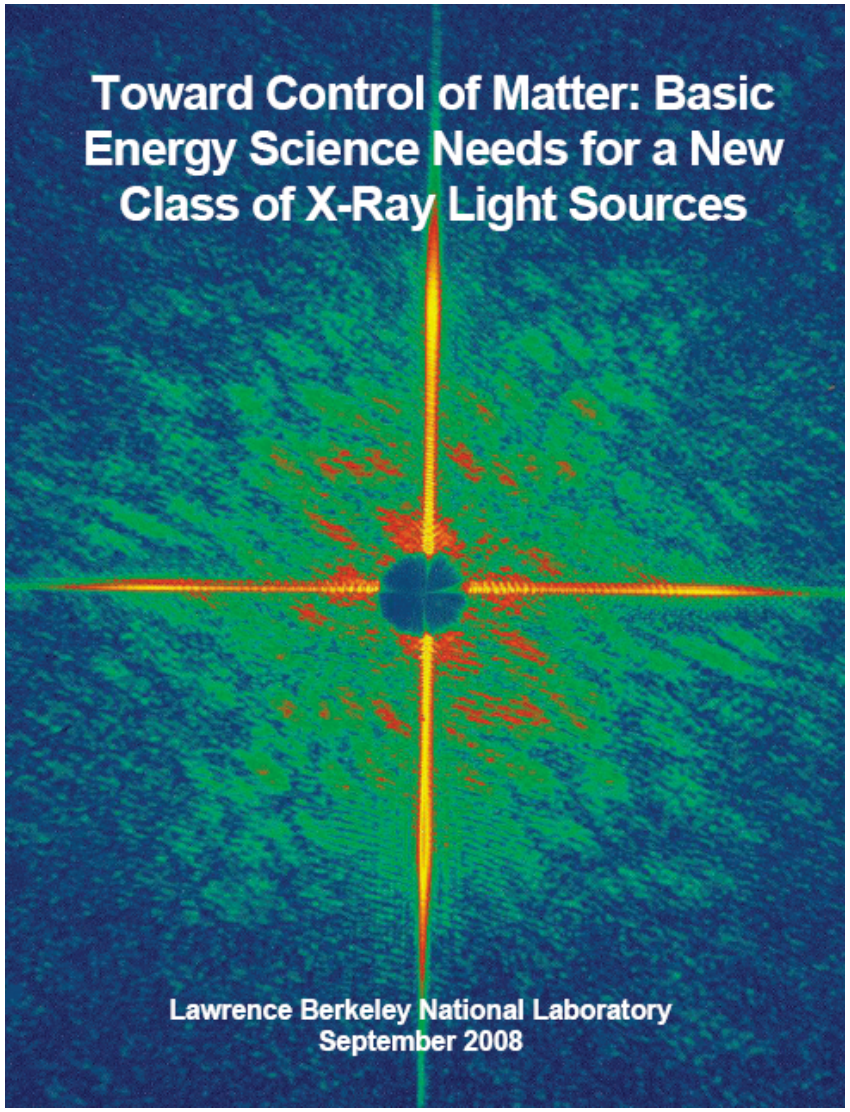

highly mature, and significant improvements in performance will be difficult to realize with this technology.

Table 1. Facility requirements derived from breakout sessions.

Property	Facility Requirements	Comments
Energy range (eV)	10–3000	Up to 1000-eV photon energy in the fundamental. Higher energies in the third harmonic, up to 3000 eV, would also be utilized, with reduced peak power.
Repetition rate (kHz)	100 or higher 1–100	High repetition rates for coincidence experiments. Lower rep-rates also have application; 1 kHz for flash imaging, 10 – 100 kHz for other imaging experiments.
Peak power (GW)	0.1–1	For 10–1000 eV, up to 10 MW from 1000–3000 eV. High peak power required for four-wave mixing and for dilute targets. 0.3 GW peak power for attosecond pulses.
Peak flux (Photons/pulse/0.1%BW)	10^{10}–10^{12} 10^{8}	10-1000 fs pulses. 0.1 fs pulses.
Average flux (Photons/s/0.1%BW)	10^{15}–10^{17} 10^{10}–10^{13}	10–1000 fs pulses. 0.1 fs pulses.
Power density (W/cm^2)	10^{14}–10^{21}	High power density for study of strong nonlinear effects. Otherwise one ionization event per shot for coincidence measurements.
Pulse length (fs)	1-1000 0.1	Control of Δt and ΔE (close to transform limit). Electron dynamics requires attosecond pulses.
Energy resolution (eV)	0.01	Control of Δt and ΔE, ~2-3 times the transform limit. Use monochromator (pinhole) when necessary.
Coherence		Full spatial coherence, close to transform limited temporal coherence.
Harmonics	1% < 0.1 %	Desirable for obtaining higher photon energies, at ~1% of the fundamental power. As low as possible; for some experiments, filter elements may be needed.
Spot size (μm)	1-100 0.05	Tunable spot size at the sample. Desirable for high-intensity AMO experiments.
Intensity stability	5%	Intensity should be recorded shot by shot.
Position stability		< 0.1σ (beam size) transverse position.
Pointing stability (μ-rad)	<10	
Background signal	<0.1 %	Contrast ratio 1:1000 desirable.
Polarization	Variable, linear/circular	
Timing stability (fs)	<5 10	Laser synchronization for pump–probe experiments. Imaging applications.

Major scientific thrusts with a soft x-ray FEL

Chemical Physics

Attosecond Manipulation of Electronic Motion

Atomic, Molecular, and Optical Physics

Electron Dynamics at the Time Scales of Atomic and Electronic Motion in Highly Excited Atoms and Molecules

Magnetization and Spin Dynamics

Magnetism at Fundamental Length and Time Scales

Correlated Materials

Emergent Phenomena due to Collective Behavior in Complex Materials

Nanoscale Dynamics and Complexity

X-Ray Imaging and X-Ray Photon Correlation Spectroscopy

https://hpcrd.lbl.gov/sxls/Workshop_Report_Final.pdf